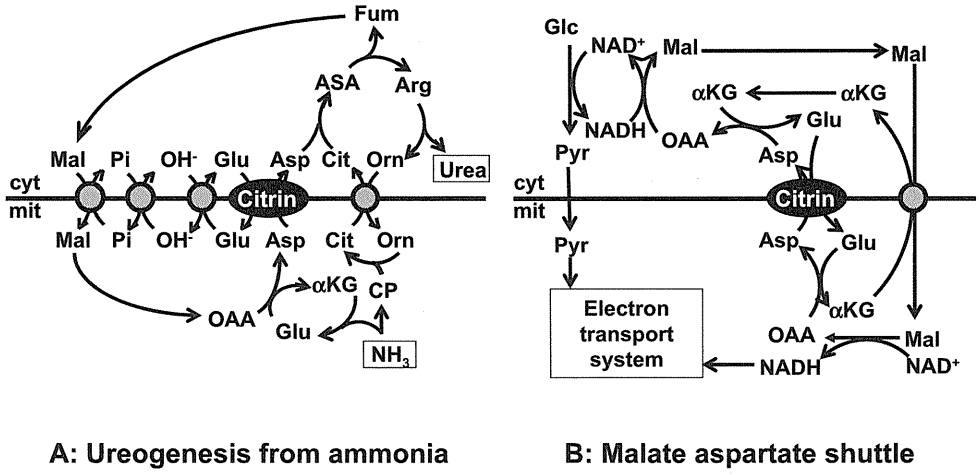

Fig. 1. Functions of citrin (liver-type AGC). (A) The role of citrin in ureogenesis from ammonia [35], and (B) the role of citrin in malate aspartate shuttle. Abbreviations are, Arg, arginine; ASA, argininosuccinate; Asp, aspartate; αKG, α-ketoglutarate; Cit, citrulline; CP, carbamoyl phosphate; cyt, cytosol; Fum, fumarate; Glc, glucose; Glu, glutamate; Mal, malate; mit, mitochondria; OAA, oxaloacetate; Orn, ornithine; Pyr, pyruvate.

Now, we propose a potentially different course of citrin deficiency (Fig. 2), because a number of Japanese subjects with citrin deficiency suffer from various kinds of disorders during the so-called "Apparently Healthy Period" [2,22–27]. There have been a few patients with NICCD that have required liver transplantation due to severe, prolonged symptoms [2,28,29], and patients presenting with CTLN2 typically continued to worsen unless also treated by liver transplantation [1,2,21,30,31]. The reason for the deterioration will be discussed later.

Characteristic food preference/food aversion of citrin-deficient subjects

It has been long known that CTLN2 patients have peculiar preference for protein- and fat-rich food, such as peanuts and soy beans. Recently, we noticed that aversion to carbohydrate-rich food, such as cooked rice and sweet things, was the other side of their food preference. Saheki et al. [32] performed nutritional assessment of 18 Japanese citrin-deficient subjects in the age ranged from 1 to 33 years old, who have been diagnosed as carrying mutation(s) in both alleles: some had suffered from NICCD, some are siblings or a father of NICCD patients, and one was at the early stage of CTLN2. The results (Fig. 3) clearly showed a marked decrease in carbohydrate intake in viewpoint of a smaller proportion of carbohydrates contributing to the total energy distribution (protein/fat/carbohydrate: PFC ratio), a reduced net intake relative to age- and sex-matched controls and a shift towards a lower centile distribution for carbohydrate intake. This unique food preference of citrin-deficient subjects is markedly different from the well-known aversion to protein among the patients with the other late-onset urea cycle enzymopathy or lysinuric protein intolerance. This unique food taste suggests some correlation of the tendency to the pathogenesis and pathophysiology of citrin deficiency.

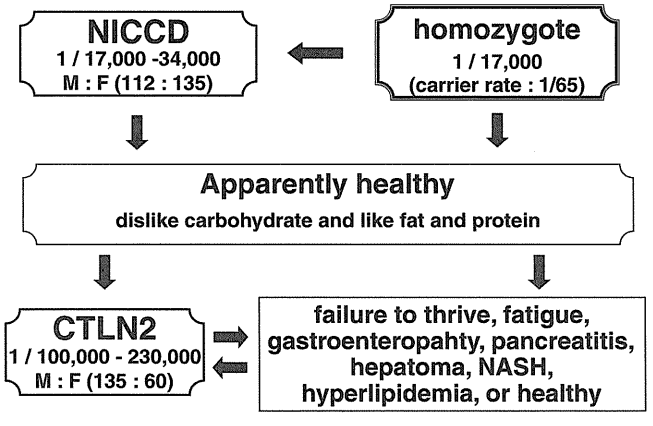

Fig. 2. Prognosis or life cycle of Japanese citrin-deficient subjects. M:F means numbers of male and female patients diagnosed. Incidence and prevalence were shown in the figure.

Carbohydrate toxicity in citrin deficiency

Tamakawa et al. [33] reported an interesting and important case with CTLN2. A 52-year-old woman fell into coma associated with hyperglycemia and hyperammonemia after receiving an infusion first composed of high dose of glucose (120 g/700 ml) and amino acids because of intractable pain and no appetite after operation for breast cancer. After recovering well, she received again a high-dose glucose infusion without amino acids. Again, she fell into coma with hyperammonemia.

Many CTLN2 patients died in a few weeks or months after infusion of glyceol composed of 10% glycerol and 5% fructose for the treatment of brain edema caused by hyperammonemia. Yazaki et al. [34] summarized reports in which the CTLN2 patients were treated with glyceol (8 cases), glyceol plus mannitol (4 cases), or mannitol (2 cases) for brain edema. All except one treated with glyceol alone or glyceol plus mannitol worsened after the treatment. Two CTLN2 patients treated with mannitol alone survived.

Concerning carbohydrate toxicity, we present a girl (P557S2) who was found to be a compound heterozygote carrying two different mutations in *SLC25A13* at 10 years old [26,32], together with her elder sister (P557) who suffered from CTLN2 and was treated with liver transplantation. Since at 13 years old, P557S2 complained of skinniness, fatigue and abdominal disorders, we examined her in connection with food intake (Figs. 3 and 4) [26,32]. As shown in Fig. 4, when she took hospital meals with high-carbohydrate energy ratios, she showed significant increases in plasma ammonia and Cit, and became drowsy. Therefore, we allowed her to take her favorite meals with fat- and protein-rich, and carbohydrate-low meals, resulting in only a slight increase in plasma ammonia with no increase in Cit. In this examination, we noticed a linear relation between plasma glucose and ammonia concentra-

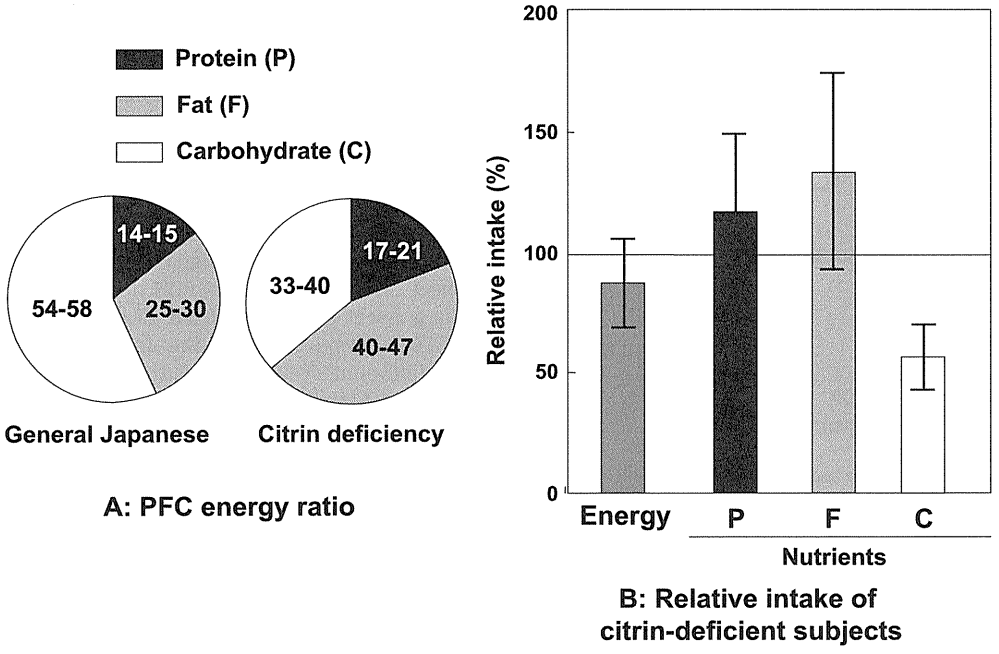

Fig. 3. Nutritional assessment of 18 citrin deficiency subjects revealed their characteristic dietary intakes. (A) Energy ratio of protein, fat and carbohydrate (PFC) of control general Japanese (left) and of citrin deficiency subjects (right), and (B) intake of energy and nutrients relative to age- and sex-matched controls [32].

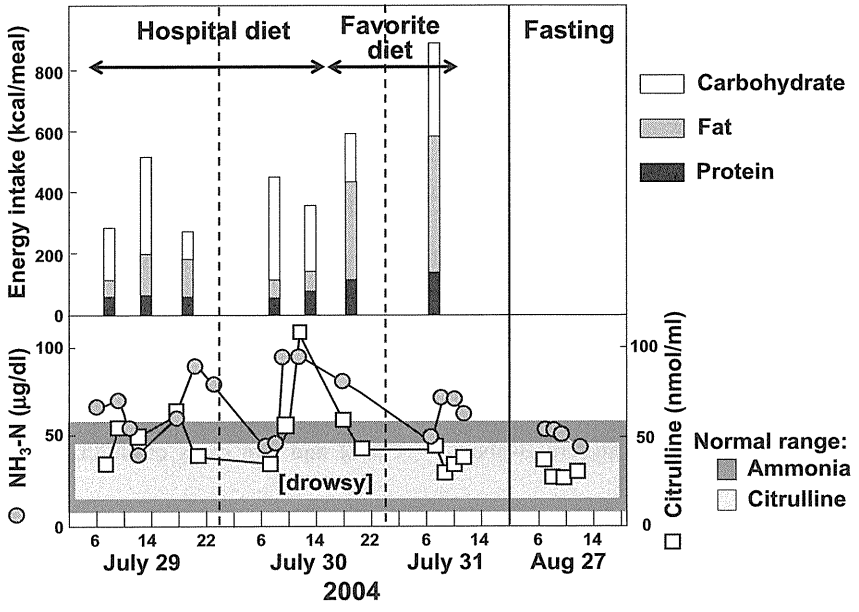

Fig. 4. Laboratory examination of 13-year-old girl (P557S2) at the early stage of CTLN2: relation between diets and plasma ammonia and citrulline. The upper panel depicts energy intake of each meal together with protein (black): fat (grey): carbohydrate (white) energy ratio. Arrows in the figure indicate duration of the hospital or her favorite meals taken. The lower panel, plasma ammonia (circle) and citrulline (square) concentrations with their control ranges (heavy and light grey, respectively).

tions after she took various kinds of breakfast (Fig. 5). All these results suggest carbohydrate toxicity in CTLN2. This can be explainable by metabolic disturbances in citrin deficiency as follows.

Ureogenesis in citrin-deficient state and its relation to carbohydrate toxicity

As described by Williamson in 1976 [35], ureogenesis under control states, liver-type AGC, citrin, plays a role in ureogenesis from ammonia as a nitrogen source (Fig. 1A). Under citrin deficiency without AGC (Fig. 6), Glu formed from ammonia, instead of Asp, goes out of mitochondria, converted to Asp by the action of cytosolic aspartate aminotransferase, and formed Asp is used for ASS reaction, indicating that urea may be synthesized in citrin deficiency. But in this metabolic pathway, oxaloacetate as an amino donor should be formed from fumarate via malate in the cytosolic compartment, which generates NADH. If the generated NADH is oxidized, urea can be synthesized under citrin deficiency. Under enhanced carbohydrate metabolism, liver plays a role in glucogenesis and fat synthesis. During the carbohydrate metabolism from glucose, fructose, glycerol and so on, NADH is formed and should be oxidized to continue aerobic glycolysis. The resultant NADH

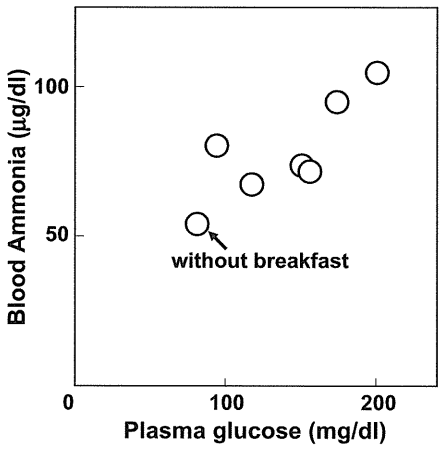

Fig. 5. Relation between plasma ammonia and glucose of a citrin-deficient patient (P557S2) after taking various kinds of breakfast. Plasma ammonia and glucose concentrations were measured 1 h and 2 h after taking various kinds of breakfast, and the maximum value of each breakfast was plotted.

accumulation or increase in NADH/NAD^+ ratio in the cytosol inhibits ureogenesis in citrin deficiency. Entry of a large amount of carbohydrate into the citrin-deficient liver may result in inhibition of glycolysis: accumulation of NADH inhibits glyceraldehyde 3-phosphate dehydrogenase and causes accumulation of glycerol 3-phosphate [data not shown], leading to the inhibition of phosphofructokinase step [36,37]. It may also cause energy deficit. These metabolic disturbances in the liver of citrin deficiency may mediate some kind of signal to the brain to avoid eating carbohydrate.

Animal model for citrin deficiency

It is important to generate animal models for elucidating the pathogenesis and pathophysiology of a disease and for developing new therapeutics based on the pathogenesis. First, we generated a citrin knockout (KO) mouse by homologous recombination to destroy *Slc25a13*. The resultant citrin KO mice were useful for analysis of ureogenesis in the perfused liver [38,39], but did not show any significant phenotype or symptoms (Table 1). This is apparently because mouse liver contains another active NADH shuttle, glycerophosphate shuttle, which consists of two glycerol 3-phosphate dehydrogenases from cytosol (cGPDH) and mitochondria (mGPDH). The citrin/mGPDH double KO mice we generated [40] revealed a number of human citrin deficiency symptoms, such as hyperammonemia under fed conditions, citrullinemia, hypoglycemia and so on (Table 1). The hepatic lactate/pyruvate ratio was high and increased by the administration of sucrose in the double KO mice. The most prominent characteristics of the mice are the hyperammonemia enhanced by the administration of sugars, confirming the carbohydrate toxicity in citrin deficiency.

Since sweet taste is a signal of an energy source, even mice like sweet taste. The citrin/mGPDH double KO mice, however, do not like a sweet taste. Mice from all genotypes (wild type, citrin KO, mGPDH KO mice) except the double KO mice voluntarily took a large amount of sucrose solution [data not shown]: namely, the double KO mice revealed a tendency similar to the citrin-deficient subjects.

Issues of the conventional treatment procedures for hyperammonemia in citrin deficiency

Some of the conventional treatment procedures for hyperammonemia may be very harmful for citrin deficiency. Low-protein and high-carbohydrate meals are standard for the therapy of urea cycle enzymopathy and lysinuric protein intolerance. Such meals, however, may cause disturbances such as hyperammonemia and hypertriglyceridemia in citrin deficiency [41]. In a similar sense, infusion of high concentration of sugar solution and glycerol solution for brain edema may cause deterioration [33,34,42]; many yet-unreported CTLN2 patients in Japan have been treated with such therapy, resulting in rapid death. Since high-carbohydrate meals are common in Japan (Fig. 3) even for hospital meals (Fig. 4), some citrin-deficient subjects should have become hyperammonemic for the first time when they were admitted to a hospital, as reported [25]. Similarly, some citrin-deficient subjects should have become ill after the entrance into primary school [26], where all schoolchildren had to take a high-carbohydrate lunch provided from school.

Possible treatment procedures for citrin deficiency

The most effective treatment procedure for citrin deficiency so far is liver transplantation [1,2,21,28–31]; more than 50 cases of CTLN2 and five cases of NICCD have been treated successfully.

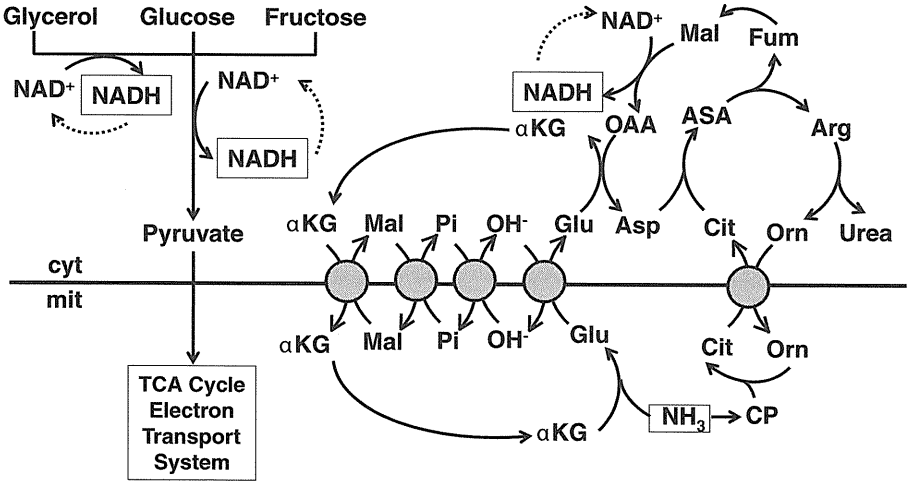

Fig. 6. Ureogenesis under citrin deficiency is inhibited by the accumulation of cytosolic NADH generated by the metabolism of carbohydrate. Abbreviations are shown in Fig. 1.

Table 1
Comparison of symptoms and laboratory examinations between CTLN2, NICCD and animal models.

Symptoms	Human citrin deficiency		Citrin KO	Citrin/mGPDH
	CTLN2	NICCD	Mice	Double KO mice
Plasma ammonia				
Under-fed state	High	+ ~ −	−	High
Under-fasted state	Normal			Normal
Plasma citrulline	High	High	Normal	High
Hypoglycemia	−	+	+/−	+
Low BMI/Growth retardation	+	+	−	+
Fatty liver	+	+	+ (fasted)	+ (fasted)
Sugar toxicity	+	+	−	+

BMI, body mass index.

After operation, they are metabolically normal, although issues are donor, cost and administration of immunosuppression drugs.

Low-carbohydrate and high-protein diets seem to be effective for NICCD and CTLN2 [41,43,44]. Doctors should not force high-carbohydrate and low-protein meals for the patients with citrin deficiency, but might have to be cautious about the protein amount in diet if the hepatic ASS activity is decreased.

Administration of arginine may be effective against hyperammonemia and hypertriglyceridemia [41,44], even though plasma arginine levels in CTLN2 patients are rather high [2]. In the experiments using the citrin/mGPDH KO mice, we recognized that administration of amino acid mixture (tryptone; casein pancreatic hydrolysate) caused no increase in blood ammonia in contrast to ornithine carbamoyl transferase-deficient spf-ash mice [45], but rather suppressed increases in blood ammonia produced by administration of sucrose solution [data not shown], suggesting that amino acid mixture or some specific amino acid(s) may inhibit the pathophysiological process.

We are now testing sodium pyruvate which oxidizes cytosolic NADH to NAD^+ by lactate dehydrogenase reaction and may provide energy as a substrate for TCA cycle. Pyruvate was able to decrease NADH/NAD^+ ratio, resulting in deinhibition of ureogenesis in the perfused liver of citrin KO mice [39]. In the first case, P557S2, the administration of sodium pyruvate together with arginine brought rapid increases in body weight and height, and significant improvement in laboratory examinations such as plasma Cit, threonine/serine ratio and serum PSTI (pancreatic secretory trypsin inhibitor) [26]. In another CTLN2 patient, the administration of sodium pyruvate brought a body weight gain and improved the liver histology [data not shown]. At least, administration of sodium pyruvate seems to delay the necessity of liver transplantation [personal communication from Dr. Yazaki]. A recent research reported by Nagasaka et al. [27] demonstrated that citrin deficiency is associated with oxidative stress even under apparently health states. The oxidative stress in citrin deficiency may result from reductive stress caused by accumulation of NADH [46], which may be ameliorated by the administration of sodium pyruvate.

Current treatment concepts for citrin deficiency

Current treatment concepts for citrin deficiency are summarized as follows:

(1) Some of conventional therapeutic procedures for hyperammonemia, such as low-protein and high-carbohydrate diets are harmful. This is because carbohydrate causes generation of cytosolic NADH, which inhibits glycolysis and energy production, and cause suppression of ureogenesis in citrin deficiency.
(2) Liver transplantation is very effective, but issues are donor and cost.
(3) Low-carbohydrate, and high-protein/-fat diets, favorites of citrin-deficient subjects, are recommendable.
(4) Some amino acids, such as arginine and some other unknown amino acids may be effective.
(5) Sodium pyruvate may be effective probably because it oxidizes NADH, relieves inhibition of glycolysis and itself supplies energy.
(6) Sodium pyruvate may also relieve oxidative stress in citrin deficiency, which remains to be solved.

Conflict of interest statement

The authors declare that there are no conflicts of interest.

References

[1] T. Saheki, K. Kobayashi, Mitochondrial aspartate glutamate carrier (citrin) deficiency as the cause of adult-onset type II citrullinemia (CTLN2) and idiopathic neonatal hepatitis (NICCD), J. Hum. Genet. 47 (2002) 333–341.
[2] K. Kobayashi, T. Saheki, Citrin deficiency, in: GeneReviews at GeneTests: Medical Genetics Information Resource [database online]. Copyright, University of Washington, Seattle. 1997–2008. Available at http://www.genetests.org.
[3] K. Kobayashi, D.S. Sinasac, M. Iijima, A.P. Boright, L. Begum, J.R. Lee, T. Yasuda, S. Ikeda, R. Hirano, H. Terazono, M.A. Crackower, I. Kondo, L.C. Tsui, S.W. Scherer, T. Saheki, The gene mutated in adult-onset type II citrullinaemia encodes a putative mitochondrial carrier protein, Nat. Genet. 22 (1999) 159–163.
[4] D. Dimmock, B. Maranda, C. Dionisi-Vici, J. Wang, S. Kleppe, G. Fiermonte, R. Bai, B. Hainline, A. Hamosh, W.E. O'Brien, F. Scaglia, L.J. Wong, Citrin deficiency, a perplexing global disorder, Mol. Genet. Metab. 96 (2009) 44–49.
[5] A. del Arco, J. Satrustegui, Molecular cloning of aralar, a new member of the mitochondrial carrier superfamily that binds calcium and is present in human muscle and brain, J. Biol. Chem. 273 (1998) 23327–23334.
[6] L. Palmieri, B. Pardo, F.M. Lasorsa, A. del Arco, K. Kobayashi, M. Iijima, M.J. Runswick, J.E. Walker, T. Saheki, J. Satrustegui, F. Palmieri, Citrin and aralar1 are Ca(2+)-stimulated aspartate/glutamate transporters in mitochondria, EMBO J. 20 (2001) 5060–5069.
[7] M. Iijima, M.A. Jalil, L. Begum, T. Yasuda, N. Yamaguchi, M.X. Li, N. Kawada, H. Endou, K. Kobayashi, T. Saheki, Pathogenesis of adult-onset type II citrullinemia caused by deficiency of citrin, a mitochondrial solute carrier protein: tissue and subcellular localization of citrin, Adv. Enzyme Regul. 41 (2001) 325–342.
[8] L. Begum, M.A. Jalil, K. Kobayashi, M. Iijima, M.X. Li, T. Yasuda, M. Horiuchi, A. del Arco, J. Satrustegui, T. Saheki, Expression of three mitochondrial solute carriers, citrin, aralar and ornithine transporter, in relation to urea cycle in mice, Biochim. Biophys. Acta 1574 (2002) 283–292.
[9] T. Saheki, K. Nakano, K. Kobayashi, Y. Imamura, Y. Itakura, M. Sase, S. Hagihara, S. Matuo, Analysis of the enzyme abnormality in eight cases of neonatal and infantile citrullinaemia in Japan, J. Inherit. Metab. Dis. 8 (1985) 155–156.
[10] K. Kobayashi, M.J. Jackson, D.B. Tick, W.E. O'Brien, A.L. Beaudet, Heterogeneity of mutations in argininosuccinate synthetase causing human citrullinemia, J. Biol. Chem. 265 (1990) 11361–11367.
[11] H.Z. Gao, K. Kobayashi, A. Tabata, H. Tsuge, M. Iijima, T. Yasuda, H.S. Kalkanoglu, A. Dursun, A. Tokatli, T. Coskun, F.K. Trefz, D. Skladal, H. Mandel, J. Seidel, S. Kodama, S. Shirane, T. Ichida, S. Makino, M. Yoshino, J.H. Kang, M. Mizuguchi, B.A. Barshop, S. Fuchinoue, S. Seneca, S. Zeesman, I. Knerr, M. Rodes, P. Wasant, I. Yoshida, L. De Meirleir, M.A. Jalil, L. Begum, M. Horiuchi, N. Katunuma, S. Nakagawa, T. Saheki, Identification of 16 novel mutations in the argininosuccinate synthetase gene and genotype-phenotype correlation in 38 classical citrullinemia patients, Hum. Mutat. 22 (2003) 24–34.
[12] T. Saheki, K. Kobayashi, I. Inoue, Hereditary disorders of the urea cycle in man: biochemical and molecular approaches, Rev. Physiol. Biochem. Pharmacol. 108 (1987) 21–68.
[13] K. Kobayashi, T. Saheki, Y. Imamura, T. Noda, I. Inoue, S. Matuo, S. Hagihara, H. Nomiyama, Y. Jinno, K. Shimada, Messenger RNA coding for argininosuccinate synthetase in citrullinemia, Am. J. Hum. Genet. 38 (1986) 667–680.
[14] K. Kobayashi, N. Shaheen, R. Kumashiro, K. Tanikawa, W.E. O'Brien, A.L. Beaudet, T. Saheki, A search for the primary abnormality in adult-onset type II citrullinemia, Am. J. Hum. Genet. 53 (1993) 1024–1030.
[15] T. Yasuda, N. Yamaguchi, K. Kobayashi, I. Nishi, H. Horinouchi, M.A. Jalil, M.X. Li, M. Ushikai, M. Iijima, I. Kondo, T. Saheki, Identification of two novel mutations in the SLC25A13 gene and detection of seven mutations in 102

patients with adult-onset type II citrullinemia, Hum. Genet. 107 (2000) 537–545.
[16] Y. Tazawa, K. Kobayashi, T. Ohura, D. Abukawa, F. Nishinomiya, Y. Hosoda, M. Yamashita, I. Nagata, Y. Kono, T. Yasuda, N. Yamaguchi, T. Saheki, Infantile cholestatic jaundice associated with adult-onset type II citrullinemia, J. Pediatr. 138 (2001) 735–740.
[17] T. Tomomasa, K. Kobayashi, H. Kaneko, H. Shimura, T. Fukusato, M. Tabata, Y. Inoue, S. Ohwada, M. Kasahara, Y. Morishita, M. Kimura, T. Saheki, A. Morikawa, Possible clinical and histologic manifestations of adult-onset type II citrullinemia in early infancy, J. Pediatr. 138 (2001) 741–743.
[18] T. Ohura, K. Kobayashi, Y. Tazawa, I. Nishi, D. Abukawa, O. Sakamoto, K. Iinuma, T. Saheki, Neonatal presentation of adult-onset type II citrullinemia, Hum. Genet. 108 (2001) 87–90.
[19] N. Yamaguchi, K. Kobayashi, T. Yasuda, I. Nishi, M. Iijima, M. Nakagawa, M. Osame, I. Kondo, T. Saheki, Screening of SLC25A13 mutations in early and late onset patients with citrin deficiency and in the Japanese population: Identification of two novel mutations and establishment of multiple DNA diagnosis methods for nine mutations, Hum. Mutat. 19 (2002) 122–130.
[20] T. Ohura, K. Kobayashi, Y. Tazawa, D. Abukawa, O. Sakamoto, S. Tsuchiya, T. Saheki, Clinical pictures of 75 patients with neonatal intrahepatic cholestasis caused by citrin deficiency (NICCD), J. Inherit. Metab. Dis. 30 (2007) 139–144.
[21] M. Kasahara, S. Ohwada, T. Takeichi, H. Kaneko, T. Tomomasa, A. Morikawa, K. Yonemura, K. Asonuma, K. Tanaka, K. Kobayashi, T. Saheki, I. Takeyoshi, Y. Morishita, Living-related liver transplantation for type II citrullinemia using a graft from heterozygote donor, Transplantation 71 (2001) 157–159.
[22] Y. Tsuboi, Y. Fujino, K. Kobayashi, T. Saheki, T. Yamada, High serum pancreatic secretory trypsin inhibitor before onset of type II citrullinemia, Neurology 57 (2001) 933.
[23] S. Ikeda, S. Kawa, Y. Takei, K. Yamamoto, H. Shimojo, K. Tabata, K. Kobayashi, T. Saheki, Chronic pancreatitis associated with adult-onset type II citrullinemia: clinical and pathological findings, Ann. Intern. Med. 141 (2004) W109–W110.
[24] M. Hachisu, Y. Oda, M. Goto, K. Kobayashi, T. Saheki, T. Ohura, S. Noma, S. Kitanaka, Citrin deficiency presenting with ketotic hypoglycaemia and hepatomegaly in childhood, Eur. J. Pediatr. 164 (2005) 109–110.
[25] J. Soeda, M. Yazaki, T. Nakata, S. Miwa, S. Ikeda, W. Hosoda, M. Iijima, K. Kobayashi, T. Saheki, M. Kojiro, S. Miyagawa, Primary liver carcinoma exhibiting dual hepatocellular-biliary epithelial differentiations associated with citrin deficiency: a case report, J. Clin. Gastroenterol. 42 (2008) 855–860.
[26] K. Mutoh, K. Kurokawa, K. Kobayashi, T. Saheki, Treatment of a citrin-deficient patient at the early stage of adult-onset type II citrullinaemia with arginine and sodium pyruvate, J. Inherit. Metab. Dis. 31 (2008), doi:10.1007/s10545-008-0752-x.
[27] H. Nagasaka, Y. Okano, H. Tsukahara, Y. Shigematsu, T. Momoi, J. Yorifuji, T. Miida, T. Ohura, K. Kobayashi, T. Saheki, K. Hirano, M. Takayanagi, T. Yorifuji, Sustaining hypercitrullinemia, hypercholesterolemia and augmented oxidative stress in Japanese children with aspartate/glutamate carrier isoform 2-citrin-deficiency even during the silent period, Mol. Genet. Metab. 97 (2009) 21–26.
[28] A. Tamamori, Y. Okano, H. Ozaki, A. Fujimoto, M. Kajiwara, K. Fukuda, K. Kobayashi, T. Saheki, Y. Tagami, T. Yamano, Neonatal intrahepatic cholestasis caused by citrin deficiency: severe hepatic dysfunction in an infant requiring liver transplantation, Eur. J. Pediatr. 161 (2002) 609–613.
[29] T. Shigeta, M. Kasahara, T. Kimura, A. Fukuda, K. Sasaki, K. Arai, A. Nakagawa, S. Nakagawa, K. Kobayashi, S. Soneda, H. Kitagawa, Liver transplantation for an infant with neonatal intrahepatic cholestasis caused by citrin deficiency using heterozygote living donor, Pediatr. Transplant. 2009 [Epub ahead of print] PMID: 19413723.
[30] S. Ikeda, M. Yazaki, Y. Takei, T. Ikegami, Y. Hashikura, S. Kawasaki, M. Iwai, K. Kobayashi, T. Saheki, Type II (adult onset) citrullinaemia: clinical pictures and the therapeutic effect of liver transplantation, J. Neurol. Neurosurg. Psychiatry 71 (2001) 663–670.
[31] R. Terada, K. Yamamoto, K. Kobayashi, K. Sakaguchi, Y. Iwasaki, T. Saheki, Y. Shiratori, Adult-onset type II citrullinemia associated with idopathic hypertriglyceridemia as a preceding feature, J. Gastroenterol. Hepatol. 21 (2006) 1634–1635.
[32] T. Saheki, K. Kobayashi, M. Terashi, T. Ohura, Y. Yanagawa, Y. Okano, T. Hattori, H. Fujimoto, K. Mutoh, Z. Kizaki, A. Inui, Reduced carbohydrate intake in citrin-deficient subjects, J. Inherit. Metab. Dis. 31 (2008) 386–394.
[33] S. Tamakawa, H. Nakamura, T. Katano, M. Yoshizawa, K. Ohtake, T. Kubota, Hyperallimentation therapy produces a comatose stae in a patient with citrullinemia, J. Jpn Soc. Intensive Care Med. 1 (1994) 37–41 (in Japanese).
[34] M. Yazaki, Y. Takei, K. Kobayashi, T. Saheki, S. Ikeda, Risk of worsened encephalopathy after intravenous glycerol therapy in patients with adult-onset type II citrullinemia (CTLN2), Int. Med. 44 (2005) 188–195.
[35] J.R. Williamson, Role of anion transport in the regulation of metabolism, in: R.W. Hanson, M.A. Mehlman (Eds.), Gluconeogenesis: Its Regulation in Mammalian Species, Wiley, New York, 1976, pp. 165–238.
[36] T.H. Claus, J.R. Schlumpf, M.R. El-Maghrabi, S.J. Pilkis, Regulation of the phosphorylation and activity of 6-phosphofructo 1-kinase in isolated hepatocytes by alpha-glycerolphosphate and fructose 2,6-bisphosphate, J. Biol. Chem. 257 (1982) 7541–7548.
[37] E. Van Schaftingen, R. Bartrons, H.G. Hers, The mechanism by which ethanol decreases the concentration of fructose 2,6-bisphosphate in the liver, Biochem. J. 222 (1984) 511–518.
[38] D.S. Sinasac, M. Moriyama, M.A. Jalil, L. Begum, M.X. Li, M. Iijima, M. Horiuchi, B.H. Robinson, K. Kobayashi, T. Saheki, L.C. Tsui, *Slc25a13*-knockout mice harbor metabolic deficits but fail to display hallmarks of adult-onset type II citrullinemia, Mol. Cell. Biol. 24 (2004) 527–536.
[39] M. Moriyama, M.X. Li, K. Kobayashi, D.S. Sinasac, Y. Kannan, M. Iijima, M. Horiuchi, L.C. Tsui, M. Tanaka, Y. Nakamura, T. Saheki, Pyruvate ameliorates the defect in ureogenesis from ammonia in citrin-deficient mice, J. Hepatol. 44 (2006) 930–938.
[40] T. Saheki, M. Iijima, M.X. Li, K. Kobayashi, M. Horiuchi, M. Ushikai, F. Okumura, X.J. Meng, I. Inoue, A. Tajima, M. Moriyama, K. Eto, T. Kadowaki, D.S. Sinasac, L.C. Tsui, M. Tsuji, A. Okano, T. Kobayashi, Citrin/mitochondrial glycerol-3-phosphate dehydrogenase double knock-out mice recapitulate features of human citrin deficiency, J. Biol. Chem. 282 (2007) 25041–25052.
[41] Y. Imamura, K. Kobayashi, T. Shibatou, S. Aburada, K. Tahara, O. Kubozono, T. Saheki, Effectiveness of carbohydrate-restricted diet and arginine granules therapy for adult-onset type II citrullinemia: a case report of siblings showing homozygous SLC25A13 mutation with and without the disease, Hepatol. Res. 26 (2003) 68–72.
[42] H. Takahashi, T. Kagawa, K. Kobayashi, H. Hirabayashi, M. Yui, L. Begum, T. Mine, S. Takagi, T. Saheki, Y. Shinohara, A case of adult-onset type II citrullinemia – deterioration of clinical course after infusion of hyperosmotic and high sugar solutions, Med. Sci. Monit. 12 (2006) CS13–CS15.
[43] D. Dimmock, K. Kobayashi, M. Iijima, A. Tabata, L.J. Wong, T. Saheki, B. Lee, F. Scaglia, Citrin deficiency: a novel cause of failure to thrive that responds to a high-protein, low-carbohydrate diet, Pediatrics 119 (2007) e773–777.
[44] K. Fukushima, M. Yazaki, M. Nakamura, N. Tanaka, K. Kobayashi, T. Saheki, H. Takei, S. Ikeda, Conventional diet therapy for hyperammonemia is risky in the treatment of hepatic encephalopathy associated with citrin deficiency, Int. Med. 49 (2010) 243–247.
[45] M.X. Li, T. Nakajima, T. Fukushige, K. Kobayashi, N. Seiler, T. Saheki, Aberrations of ammonia metabolism in ornithine carbamoyltransferase-deficient spf-ash mice and their prevention by treatment with urea cycle intermediate amino acids and an ornithine aminotransferase inactivator, Biochim. Biophys. Acta 1455 (1999) 1–11.
[46] H. Jaeschke, C. Kleinwaechter, A. Wendel, NADH-dependent reductive stress and ferritin-bound iron in allyl alcohol-induced lipid peroxidation in vivo: the protective effect of vitamin E, Chem. Biol. Interact. 81 (1992) 57–68.

Molecular Genetics and Metabolism 104 (2011) 492–500

Contents lists available at SciVerse ScienceDirect

Molecular Genetics and Metabolism

journal homepage: www.elsevier.com/locate/ymgme

Metabolomic analysis reveals hepatic metabolite perturbations in citrin/mitochondrial glycerol-3-phosphate dehydrogenase double-knockout mice, a model of human citrin deficiency

Takeyori Saheki [a,*,1], Kanako Inoue [a], Hiromi Ono [a], Anmi Tushima [a], Natsumi Katsura [a], Mana Yokogawa [a], Yukari Yoshidumi [a], Tomiko Kuhara [b], Morimasa Ohse [b], Kazuhiro Eto [c], Takashi Kadowaki [d], David S. Sinasac [e,f], Keiko Kobayashi [g]

[a] Institute for Health Sciences, Tokushima Bunri University, 180 Yamashiro-cho, Tokushima, 770–8514 Japan
[b] Medical Research Institute, Kanazawa Medical University, Uchinada, 920–0293, Japan
[c] Department of Internal Medicine, School of Medicine, Teikyo University, Tokyo 173–8605, Japan
[d] Department of Internal Medicine, Graduate School of Medicine, University of Tokyo, Tokyo 113–8655, Japan
[e] Biochemical Genetics Laboratory, Alberta Children's Hospital, Calgary, Alberta, Canada T3B 6A8
[f] Department of Medical Genetics, University of Calgary, Calgary, Alberta, Canada T2N 4N1
[g] Kagoshima University Graduate School of Medical Dental Sciences, Kagoshima, 890–8544, Japan

ARTICLE INFO

Article history:
Received 28 July 2011
Received in revised form 14 August 2011
Accepted 14 August 2011
Available online 19 August 2011

Keywords:
Citrin
Adult-onset type II citrullinemia (CTLN2)
Glycerol-3-phosphate
Citrulline
Sodium pyruvate

ABSTRACT

The citrin/mitochondrial glycerol-3-phosphate dehydrogenase (mGPD) double-knockout mouse displays phenotypic attributes of both neonatal intrahepatic cholestasis and adult-onset type II citrullinemia, making it a suitable model of human citrin deficiency. In the present study, we investigated metabolic disturbances in the livers of wild-type, citrin (Ctrn) knockout, mGPD knockout, and Ctrn/mGPD double-knockout mice following oral sucrose versus saline administration using metabolomic approaches. By using gas chromatography/mass spectrometry and capillary electrophoresis/mass spectrometry, we found three general groupings of metabolite changes in the livers of the double-knockout mice following sucrose administration that were subsequently confirmed using liquid chromatography/mass spectrometry or enzymatic methods: a marked increase of hepatic glycerol 3-phosphate, a generalized decrease of hepatic tricarboxylic acid cycle intermediates, and alterations of hepatic amino acid levels related to the urea cycle or lysine catabolism including marked increases in citrulline and lysine. Furthermore, concurrent oral administration of sodium pyruvate with sucrose ameliorated the hyperammonemia induced by sucrose, as had been shown previously, as well as almost completely normalizing the hepatic metabolite perturbations found. Overall, we have identified additional metabolic disturbances in double-KO mice following oral sucrose administration, and provided further evidence for the therapeutic use of sodium pyruvate in our mouse model of citrin deficiency.

1. Introduction

In 1999, Kobayashi et al. [1] found that adult-onset type II citrullinemia (CTLN2) – a late-onset form of citrullinemia characterized by disturbances of consciousness, hyperammonemia and cerebral edema leading to death – is caused by mutations in the *SLC25A13* gene that encodes the mitochondrial solute carrier citrin. Citrin, and the closely related protein aralar (encoded by *SLC25A12*), were subsequently both found to be aspartate (Asp)–glutamate (Glu) carriers (AGC) by Palmieri et al. in 2001 [2]. Based on their mRNA and protein expression patterns, citrin is considered the liver-type AGC isoform, while aralar the brain- and skeletal muscle-type AGC isoform [3,4]. Also in 2001, three groups reported that mutations in *SLC25A13* cause not only CTLN2, but also a form of neonatal hepatitis characterized by intrahepatic cholestasis. This latter presentation was dubbed "intrahepatic

Abbreviations: AASS, α-aminoadipate δ-semialdehyde synthase; AGC, aspartate–glutamate carrier; αKG, α-ketoglutarate; ANOVA, analysis of variance; Ala, alanine; Arg, arginine; ASA, argininosuccinate; Asp, aspartate; ASS, argininosuccinate synthetase; CE/MS, capillary electrophoresis/mass spectrometry; CTLN2, adult-onset type II citrullinemia; Ctrn-KO, *Slc25a13* (citrin) knockout; DHAP, dihydroxyacetone phosphate; GC/MS, gas chromatography/mass spectrometry; Gln, glutamine; Glu, glutamate; G3P, glycerol-3-phosphate; KO, knockout; Lac, lactate; LC/MS, liquid chromatography/mass spectrometry; Lys, lysine; mGPD, mitochondrial glycerol-3-phosphate dehydrogenase; Na, sodium; NAD^+, nicotinamide adenine dinucleotide, oxidized; NADH, nicotinamide adenine dinucleotide, reduced; NICCD, neonatal intrahepatic cholestasis caused by citrin deficiency; Orn, ornithine; Pyr, pyruvate; TCA, tricarboxylic acid; wt, wild-type.

* Corresponding author at: Institute of Resource Development and Analysis, Kumamoto University, 2-2-1 Honjo, Kumamoto 860–0811 Japan. Fax: +81 96 373 6599.
E-mail address: takesah@kumamoto-u.ac.jp (T. Saheki).
[1] Present address: Institute of Resource Development and Analysis, Kumamoto University, Kumamoto, 860–0811 Japan.

1096-7192/$ – see front matter © 2011 Elsevier Inc. All rights reserved.
doi:10.1016/j.ymgme.2011.08.015

cholestasis caused by citrin deficiency" (NICCD) [5–7]; and as a result, a new disease entity, "citrin deficiency", was established to encompass both age-dependent disease presentations [8]. With more and more citrin-deficient patients being identified as a result of increased awareness of the disorder (especially outside of Japan), the availability of molecular diagnostic testing, and expanded newborn screening programs, it is now clear that the clinical features of citrin deficiency are expanding. In addition to the initially described features of NICCD and CTLN2, citrin deficiency also now appears to lead to additional consequences throughout life: growth retardation and fatty liver in infancy; elevated cholesterol, hypertriglyceridemia and pancreatitis in late childhood and adolescence; and an increased risk of hepatocellular carcinoma in adults [8–20]. This newly recognized pediatric presentation of citrin deficiency, following the resolution of NICCD symptoms, has recently been dubbed "failure to thrive and dyslipidemia caused by citrin deficiency" or FTTDCD [21].

The wide variety of symptoms associated with citrin deficiency is predicted to result directly from the loss of citrin's function as an AGC. The liver AGC is not only important for the synthesis of proteins, nucleotides and urea through its translocation of mitochondrial Asp into the cytosol, but also plays an indispensable role in cytosolic NADH metabolism as a member of malate-Asp shuttle. Gluconeogenesis from lactate (Lac) also requires the liver AGC to maintain the stoichiometry of NADH, as originally predicted by Krebs et al. [22]. One of the most unusual features of citrin deficiency is that all patients tested to date show a unique food predilection; they dislike carbohydrate-rich foods and prefer protein- and fat-rich foods [8,9]. A detailed nutritional assessment of 18 Japanese citrin-deficient patients (ranging from 1 to 33 years of age) clearly demonstrated a significant reduction in their intake of carbohydrates, with compensatory increases in protein and fat, compared to established age- and gender-matched norms for the general Japanese population [23].

In an attempt to model citrin deficiency in mice, our initial studies of the homologous-recombination-generated Slc25a13-knockout (KO) mouse demonstrated metabolic perturbations in many of the pathways in which citrin is predicted to play a role, using both *in vitro* assays and liver perfusion experiments [24,25]. Despite these findings, however, the mice failed to exhibit overt phenotypes relevant to human citrin deficiency. Based on a published report [26] and our own unpublished data that rodent liver contains much higher levels of glycerol-phosphate shuttle activity than human liver, we have now established a more representative model of human citrin deficiency [27] through breeding *Slc25a13*-KO (Ctrn-KO) mice with *Gpd2*-KO (a.k.a. mitochondrial glycerol-3-phosphate dehydrogenase or mGPD) mice, to create Ctrn/mGPD double-KO mice. The double-KO mouse shows a sustained elevation of plasma citrulline, hyperammonemia under fed conditions, as well as hypoglycemia and fatty liver under fasted conditions — all phenotypic features reminiscent of human citrin deficiency. Furthermore, one of the most prominent characteristics of the double-KO mouse is exacerbated hyperammonemia following oral sucrose administration [26], which provides a hypothesis for why citrin-deficient patients avoid carbohydrate-rich foods.

In this study, we have focused on examining the metabolic disturbances present in the livers of wild-type (wt), Ctrn-KO, mGPD-KO and double-KO mice following oral saline (as a control) or sucrose administration using a metabolomic approach. Gas chromatography/mass spectrometry (GC/MS) and capillary electrophoresis/mass spectrometry (CE/MS) were used to identify untargeted metabolites that were specifically altered in the livers of the double-KO mice following oral sucrose administration, and these findings were subsequently confirmed using either enzymatic methods or liquid chromatography/mass spectrometry (LC/MS) amino acid analysis for the quantitation of specific metabolites. We also show that sodium (Na) pyruvate (Pyr), which had been used previously to ameliorate the hyperammonemia resulting from liver perfusion of ammonium chloride in Ctrn-KO mice, also has a therapeutic effect on the metabolic disturbances in the liver of the double-KO mice that are induced by oral sucrose administration.

2. Methods and materials

2.1. Animals

All wt, Ctrn-KO, mGPD-KO and Ctrn/mGPD double-KO mice used in this study were congenic on the C57BL/6J background. Mice used in the experiments were generated using the breeding scheme described previously by Saheki et al. [27]. Briefly, mGPD-KO and double-KO mice were obtained by mating heterozygous Ctrn-KO/homozygous mGPD-KO (i.e., $Ctrn^{+/-}/mGPD^{-/-}$) mice, while wt and Ctrn-KO mice were generated by mating heterozygous Ctrn-KO (i.e., $Ctrn^{+/-}/mGPDH^{+/+}$) mice. Genotyping was performed with DNA extracted from ear punches using procedures specific for each of the targeted mutations in the Ctrn-KO [24] and mGPD-KO [28] mice, respectively.

2.2. Animal care

Mice were maintained at a constant temperature (23 ± 1 °C) on a 12-hour light (7 am to 7 pm)/dark cycle with free access to water and CE2CE-2 chow (25% protein, 4.6% fat, and 50% carbohydrate providing 343 kcal/100 g; CLEA Japan, Tokyo, Japan). The mice used for the experiments were analyzed between 80 and 150 days of age.

In the experiments to examine the metabolic alterations in liver extracts, fed mice were sacrificed between 11 am and 12 am by cervical dislocation, 1 h after oral administration of either 0.9% saline or 50% sucrose (10 g/kg body weight) at a standard dose of 20 ml/kg via gastric tube.

This study was approved by the Committee for Animal Experimentation at Tokushima Bunri University.

2.3. Preparation of liver extracts and blood samples

Livers were quickly removed, freeze-clamped between aluminum tongues, pulverized under liquid nitrogen and homogenized in 3% perchloric acid. Following the centrifugation of the samples at $10,000 \times g$ for 20 min at 4 °C, the supernatants were neutralized with 1 M Na bicarbonate and used for GC/MS, enzymatic analysis or amino acid analyses, as described subsequently. For the CE/MS analysis, livers were pulverized in liquid nitrogen and homogenized in methanol containing internal standards (1 ml per 100 mg liver) supplied by Human Metabolome Technologies Inc. (Tsuruoka, Yamagata, Japan). Liver extracts from four mice of the same genotype and treatment were then combined on an equivalent per liver weight basis and analyzed as single samples, for a total of eight samples analyzed.

In the experiments to examine the effects of Na-Pyr, blood was taken from the heart under somnopentyl anesthesia (64.8 mg Na pentobarbital/kg body weight) 1 h after oral administration of either 25% sucrose (5 g/kg body weight) in saline or 25% sucrose in 1 M Na-Pyr (Musashino Chemicals Laboratory, Tokyo, Japan) and assayed for blood ammonia. Livers were removed and treated as described earlier for the determination of hepatic metabolite levels.

2.4. Analytical procedures

The GC/MS-based metabolomic analysis of liver homogenates was generally performed as described previously [29,30]. To 50 μl of a solution prepared from each liver extract, 50 μl of water and 900 μl of ethanol containing internal standards (2,2-dimethylsuccinate, 2-hydroxyundecanoate, D3-leucine and D4-tyrosine) were added, then the preparation was mixed and centrifuged. The supernatant was then dried under nitrogen gas and derivatized using trimethylsilylation. The GC/MS analysis was then performed as previously reported [30]. The CE/MS analysis was performed by Human Metabolome Technologies Inc. (Tsuruoka, Yamagata, Japan) as previously reported [31].

The hepatic concentrations of glycerol-3-phosphate (G3P), dihydroxyacetone phosphate (DHAP), Pyr, citrate, malate, and α-

ketoglutarate (αKG) were determined using established enzymatic methods [32–37]. Lactate was determined using the Determiner LA kit (Kyowa Medix Co. Ltd., Tokyo, Japan). Blood ammonia was assayed using the Wako Ammonia test kit (Wako Pure Chemical Industries, Osaka, Japan).

Hepatic amino acids were determined by LC/MS/MS (Acquity UPLC/TQD; Waters, Milford, MA, USA) after solid phase extraction followed by derivatization [38] using EZ:faast Amino Acid Analysis kit (Phenomenex Ltd., Los Angeles, CA, USA).

2.5. Statistical analysis

The difference between two group means was evaluated using the Student's *t*-test, with a threshold for statistical significance of $p<0.05$. Differences among multiple group means were initially evaluated using a one-way analysis of variance (ANOVA) followed by the Tukey–Kramer test, with a threshold for statistical significance of $p<0.05$.

3. Results

3.1. GC/MS-based metabolomic analysis of mouse liver extracts following oral administration

We have shown previously that the hyperammonemia observed in the fed state of Ctrn/mGPD double-KO mice is further aggravated by oral sucrose administration (50% w/v of water; 10 g/kg body weight) [27]. To investigate the metabolic perturbations associated with oral sucrose administration in the Ctrn/mGPD double-KO mice, saline (20 ml/kg body weight; used as a control) or a 50% sucrose solution (10 g/kg body weight) was administered to wt, Ctrn-KO, mGPD-KO and double-KO mice. One hour after administration, liver extracts were prepared and analyzed using GC/MS. Most strikingly, we found that hepatic G3P was markedly and specifically increased in the double-KO mice following oral sucrose administration (data not shown). We also observed lower hepatic Asp and alanine (Ala) in the double-KO mice, as well as lower hepatic tricarboxylic acid (TCA) cycle intermediates including isocitrate, succinate, fumarate and malate in Ctrn-KO, mGPD-KO and double-KO mice (data not shown). These latter findings, however, were found not only after oral sucrose administration, but also after oral saline administration.

3.2. CE/MS-based metabolomic analysis of mouse liver extracts following oral administration

In order to examine a broader range of metabolites as well as to more sensitively identify differences between oral saline versus sucrose administration among the four different mouse genotypes, we further analyzed mouse liver extracts using CE/MS. For this analysis, eight samples were analyzed using CE/MS that were from each of the four genotypes treated with either oral saline or sucrose solution, with each sample consisting of four liver extracts from mice of the same genotype receiving the same treatment. Using this approach, we found three general groupings of metabolic disturbances in the livers of the mice: G3P (as part of the glycolytic pathway), TCA cycle intermediates, and amino acids that include both urea cycle intermediates as well as other amino acids related to lysine (Lys) catabolism.

A comparison of hepatic G3P and TCA cycle intermediates among the four mouse genotypes following saline and sucrose administration, all relative to wt saline levels, is shown in Fig. 1. The CE/MS-based metabolomic analysis revealed relatively increased hepatic G3P in Ctrn-KO and double-KO mice following oral saline administration (Fig. 1A), while hepatic G3P was markedly increased in the livers of the double-KO mice following oral sucrose administration (Fig. 1B; consistent with GC/MS findings). In addition, relatively smaller increases in hepatic G3P were also observed for wt, Ctrn-KO and mGPD-KO mice following oral sucrose administration. On the other hand, the TCA cycle intermediates

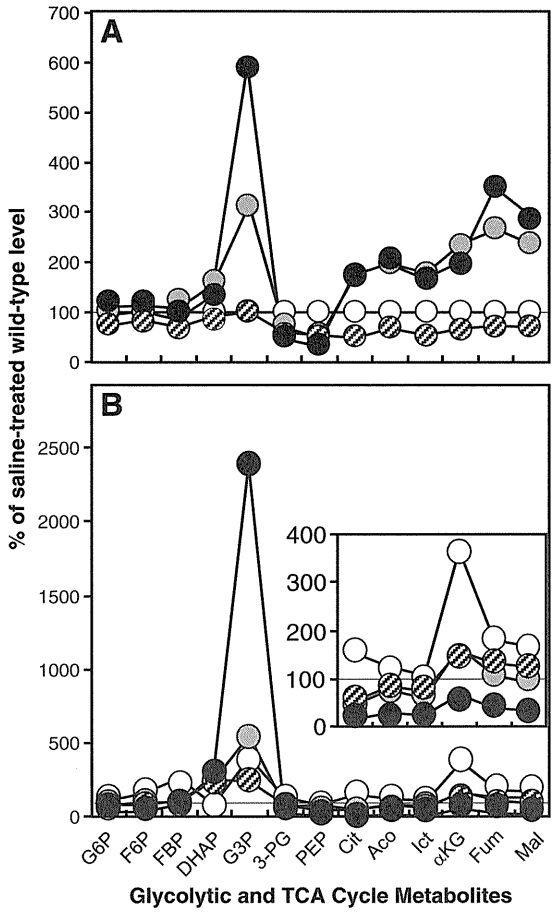

Fig. 1. Relative differences in hepatic glycolytic and TCA cycle metabolites among the mouse genotypes following oral saline (A) or sucrose administration (B), as determined by CE/MS-based metabolomic analysis. The hepatic metabolites from each genotype are expressed as the percent of saline-treated wt mice. White circles denote wt; grey, Ctrn-KO; hatched, mGPD-KO; and black, double-KO mice. The insert in (B) shows a magnification of the data specifically for the TCA cycle intermediates. Abbreviations used are G6P, glucose-6-phosphate; F6P, fructose-6-phosphate; FBP, fructose -1,6-bisphosphate; DHAP, dihydroxyacetone phosphate; G3P, glycerol-3-phosphate; 3PG, 3-phosphoglycerate; PEP, phosphoenolpyruvate; Cit, citrate; Aco, cis-aconitate; Ict, isocitrate; αKG, α-ketoglutarate; Fum, fumarate; Mal, malate.

were all relatively elevated in Ctrn-KO and double-KO mice following oral saline administration when compared to wt and mGPD-KO mice (Fig. 1A), while only the TCA cycle intermediates in the double-KO mice showed a generalized decrease compared to the other genotypes following oral sucrose administration (Fig. 1B insert).

The CE/MS-based metabolomic analysis also revealed relative changes in the urea cycle intermediates, with markedly increased hepatic citrulline and decreased hepatic ornithine (Orn) and arginino-succinate (ASA) in the double-KO mice following oral sucrose administration (Fig. 2A). Additionally, hepatic N^6-acetyl-lysine and Lys were also increased in the double-KO mice following oral sucrose administration, while saccharopine and aminoadipic acid were decreased in the double-KO mice following oral sucrose administration (Fig. 2B). The CE/MS analysis also suggests that there were no marked changes in the other amino acids, which was confirmed by amino acid analysis by LC/MS, as described later.

3.3. Confirmation of altered metabolites in mouse liver extracts using independent methods

One of the most striking findings from both the GC/MS- and CE/MS-based metabolomic approaches was the marked increase of hepatic G3P in the double-KO mice following oral sucrose administration. Using an

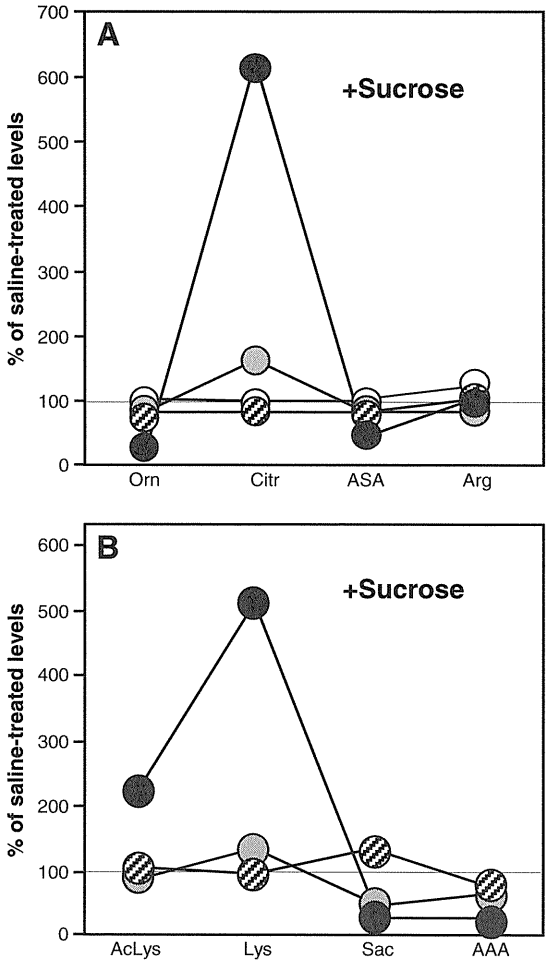

Fig. 2. Relative differences in hepatic urea cycle (A) and lysine catabolic (B) metabolites among the mouse genotypes following oral sucrose administration, as determined by CE/MS-based metabolomic analysis. The hepatic metabolites following oral sucrose administration are expressed as the percent of saline-treated levels within each of the mouse genotypes. Abbreviations used are Orn, ornithine; Citr, citrulline; ASA, argininosuccinate; Arg, arginine in (A); and AcLys, N^6-acetyl-lysine; Sac, saccharopine; and AAA, aminoadipic acid in (B).

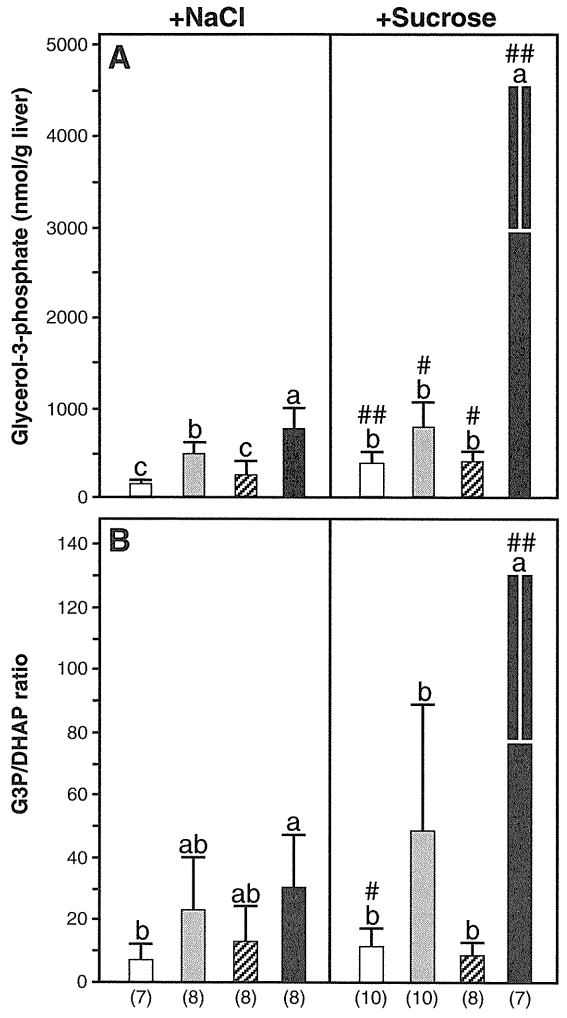

Fig. 3. Hepatic glycerol-3-phosphate (G3P; A) and G3P/DHAP ratio (B) among the four mouse genotypes following oral saline or sucrose administration. Saline (NaCl) or sucrose (10 g/kg body weight) was orally administered to the mice, as described in the Methods and materials. White bars denote wt; grey, Ctrn-KO; hatched, mGPD-KO; and black, double-KO mice. Data from each group of mice are expressed as mean ± SD. Parentheses denote the number of mice in each genotype examined. Differences among the genotypes within the same treatment group were evaluated by ANOVA followed by the Tukey–Kramer test, where mean values with the same character are not statistically different. Differences between two treatment groups within the same genotype were evaluated using a Student's *t*-test, where # denotes a statistical difference at $p<0.05$ and ## at $p<0.01$.

enzymatic method to quantitate hepatic G3P in wt, Ctrn-KO, mGPD-KO and double-KO mice, we found that the double-KO mice had a mean hepatic G3P content of 4540 nmol/g liver following oral sucrose administration (Fig. 3A). Furthermore, this concentration was significantly greater than that of the double-KO mice following saline administration (770 nmol/g liver; $p<0.01$, *t*-test), and each of the other genotypes following sucrose administration ($p<0.05$ in each case, ANOVA; Fig. 3A). Other smaller differences were found in hepatic G3P contents, confirming the CE/MS-based observations that each of the remaining three genotypes showed increased hepatic G3P contents when comparing oral sucrose versus saline administration (Fig. 3A), as well as higher hepatic G3P contents in the Ctrn-KO and double-KO mice compared with wt and mGPD-KO mice following oral saline administration (Fig. 3A). Using an enzymatic method to quantitate hepatic DHAP, the increased hepatic G3P found in the double-KO mice following oral sucrose administration was not accompanied by a concomitant increase in DHAP (data not shown), normally thought to be in equilibrium with G3P. As a result, a significant increase in the G3P/DHAP ratio was observed in the livers of the double-KO mice following sucrose administration (Fig. 3B). Again, smaller but statistically significant changes were also seen in G3P/DHAP ratios between double-KO and wt mice following saline administration, as well as between wt mice when comparing oral sucrose versus saline administration (Fig. 3B).

The changes observed in the TCA cycle intermediates by CE/MS were also largely confirmed using enzymatic methods for citrate, αKG and malate (Figs. 4A, B and C). Although there were no statistically significant differences in hepatic citrate between double-KO and wt mice following saline administration (as initially found by CE/MS), both Ctrn-KO and double-KO mice showed significant reductions in hepatic citrate following sucrose administration (Fig. 4A). Similar findings were also observed for αKG and malate, where Ctrn-KO and double-KO mice tended to show higher liver concentrations than wt and mGPD-KO mice following oral saline administration, but reduced levels following oral sucrose administration (the change in αKG when comparing oral saline versus sucrose administration failed to reach statistical significance for Ctrn-KO mice). Interestingly, a significant decrease in citrate, and increase in malate, were also found in wt mice when comparing saline versus sucrose administration (Figs. 3A and C), as was a significant increase in αKG in mGPD-KO mice (Fig. 3B). These latter findings were not initially found by CE/MS.

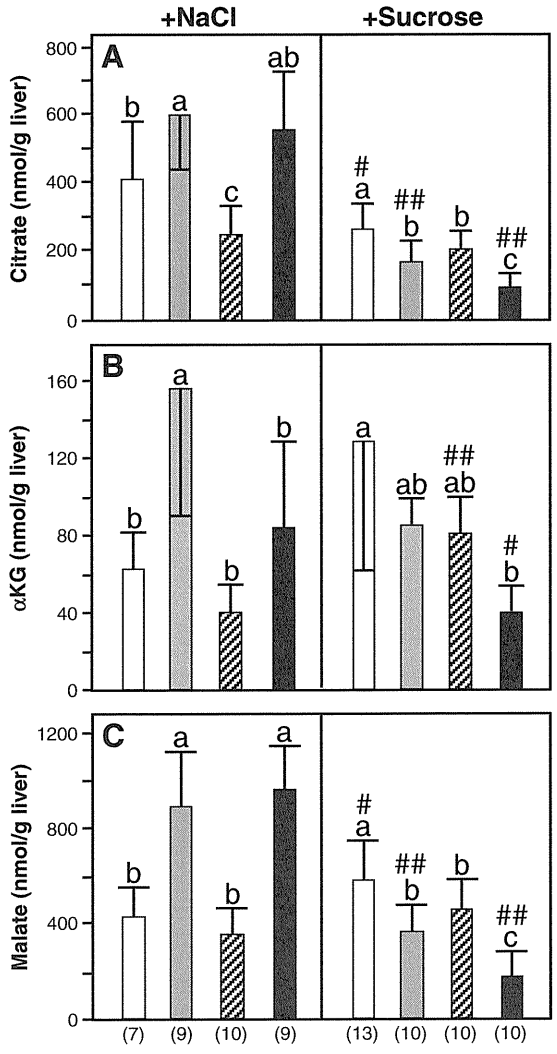

Fig. 4. Hepatic concentrations of citrate (A), α-ketoglutarate (αKG; B) and malate (C) among the four mouse genotypes following oral saline or sucrose administration. Experimental and statistical details are given in the legend of Fig. 3. White bars denote wt; grey, Ctrn-KO; hatched, mGPD-KO; and black, double-KO mice. Data from each group of mice are expressed as mean ± SD. Numbers in parentheses denote the number of mice in each genotype examined.

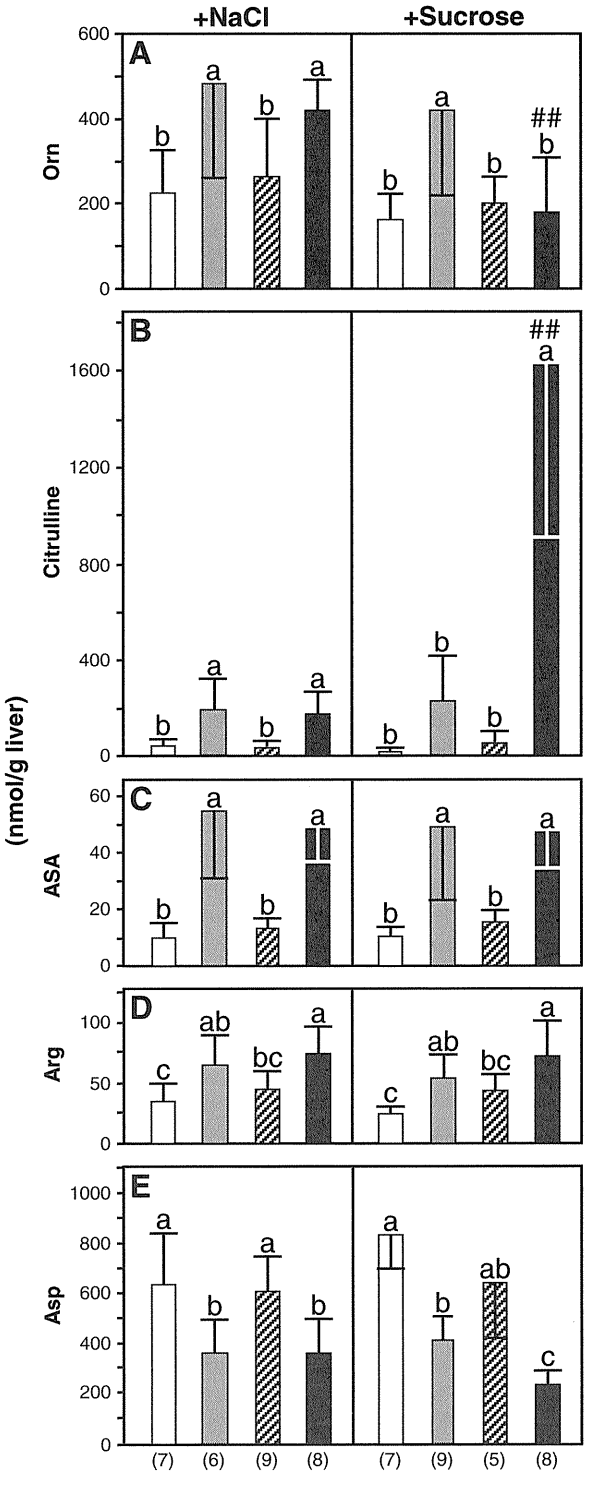

Fig. 5. Hepatic concentrations of ornithine (Orn; A), citrulline (B), argininosuccinate (ASA; C), arginine (Arg; D) and aspartate (Asp; E) among the four mouse genotypes following oral saline or sucrose administration. Experimental and statistical details are given in the legend of Fig. 3. White bars denote wt; grey, Ctrn-KO; hatched, mGPD-KO; and black, double-KO mice. Data from each group of mice are expressed as mean ± SD. Numbers in parentheses denote the number of mice in each genotype examined.

The last grouping of metabolite changes found through the metabolomic analyses were in hepatic amino acids levels. An LC/MS-based amino acid analysis (Figs. 5–7) also largely confirmed the results found by CE/MS. For the urea cycle intermediates, decreased Orn (Fig. 5A) and markedly increased citrulline (Fig. 5B) were found in the double-KO mice following sucrose versus saline administration, while higher hepatic Orn and citrulline concentrations in Ctrn-KO mice appeared independent of oral administration (Figs. 5A and B). Although hepatic ASA in the double-KO mice seemed to be lower following sucrose versus saline administration by CE/MS, ASA (Fig. 5C), arginine (Arg; Fig. 5D) and Asp (Fig. 5E) levels were all found to be unchanged by LC/MS within each genotype when comparing saline versus sucrose administration despite higher hepatic ASA and Arg, and lower hepatic Asp, in Ctrn-KO and double-KO mice relative to wt and mGPD-KO mice.

Regarding the observed changes in the other amino acids identified by CE/MS, hepatic Lys was confirmed to be specifically increased in double-KO mice following sucrose administration (Fig. 6). Hepatic Ala (Fig. 7A) was also found to be increased in wt and mGPD-KO mice following sucrose versus saline administration, Glu decreased in Ctrn-KO and double-KO mice following sucrose versus saline administration, and Gln increased in wt but decreased in double-KO mice, following sucrose versus saline administration. No further differences in other hepatic amino acids, including the ratios of the branched-chain amino acids/aromatic amino acids or threonine/serine, were detected (data not shown).

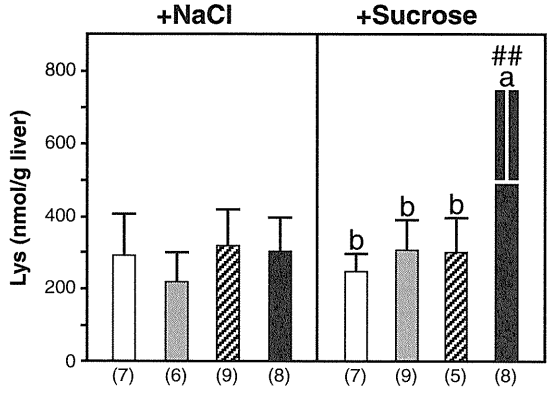

Fig. 6. Hepatic concentration of Lys among the four mouse genotypes following oral saline or sucrose administration. Experimental and statistical details are given in the legend of Fig. 3. White bars denote wt; grey, Ctrn-KO; hatched, mGPD-KO; and black, double-KO mice. Data from each group of mice are expressed as mean ± SD. Numbers in parentheses denote the number of mice in each genotype examined.

3.4. Effect of Na-Pyr on the metabolite changes induced by sucrose administration

We also tested whether Na-Pyr, which had been shown previously to ameliorate the block in ureogenesis from ammonium chloride during liver perfusion of Ctrn-KO mice [24], would also affect the metabolite changes found in the double-KO mice following sucrose administration *in vivo*. As shown in Fig. 8, the increased blood ammonia found in the double-KO mice following oral sucrose administration (5 g/kg body weight), was completely normalized to the level of littermate mGPD-KO mice when simultaneously administered with Na-Pyr (20 mmol/kg). Furthermore, increased hepatic G3P, citrulline and Lys were also largely normalized to the levels of saline-treated wt mice (Figs. 9A, C and D), while decreased hepatic citrate was increased to that of saline-treated wt mice (Fig. 9B). Overall, these findings further substantiate our previously proposed rationale for the use of Na-Pyr as a therapy for citrin deficiency.

4. Discussion

We showed previously that Ctrn/mGPD double-KO mice recapitulate many features of human citrin deficiency: growth restriction, hypoglycemia, hyperammonemia (under fed conditions), fatty liver, elevated plasma citrulline and an elevated plasma threonine/serine ratio [27]. In addition, we also found that the double-KO mice show a worsening of the hyperammonemia, a decreased Fischer ratio (i.e., plasma branched-chain amino acids/aromatic amino acids) and lower plasma Ala following oral sucrose administration. It was these latter findings which suggested that increased sucrose metabolism could exacerbate urea cycle dysfunction in double-KO mice, and that this phenomenon may underlie the aversion of citrin-deficient patients to carbohydrate-rich foods. This therefore led us to investigate the hepatic perturbations in double-KO mice following an oral sucrose administration. In the present study, we analyzed the metabolite profiles of liver extracts from wt, Ctrn-KO, mGPD-KO and double-KO mice 1 h following either an oral saline or sucrose administration, using untargeted metabolomic approaches by GC/MS and CE/MS.

The most striking finding, the markedly increased hepatic G3P content in double-KO mice following sucrose administration, was found by both GC/MS and CE/MS analyses and confirmed using an established enzymatic method. Furthermore, the increased hepatic G3P was not accompanied by a concomitant increase in DHAP, and thus led to a substantial elevation of the G3P/DHAP ratio which probably reflected an increased cytosolic NADH/NAD^+ ratio due to the lack of both malate-Asp and glycerophosphate shuttle activities. An increased cytosolic NADH/NAD^+ ratio generated from the glyceraldehyde-3-phosphate

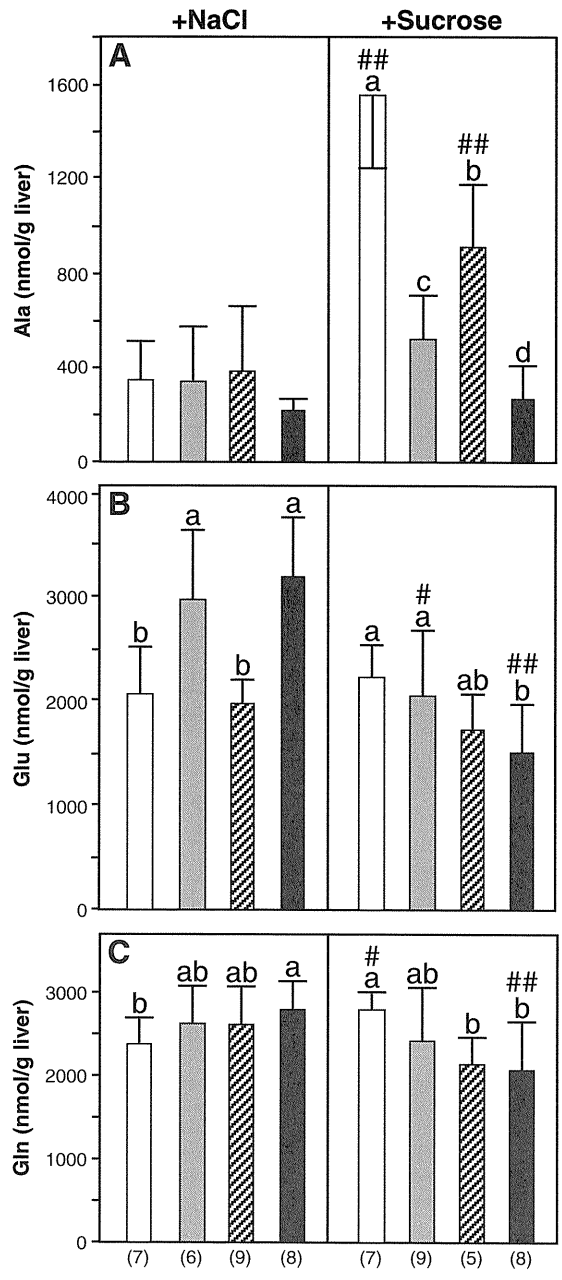

Fig. 7. Hepatic concentrations of alanine (Ala; A), glutamate (Glu; B) and glutamine (Gln; C) among the four mouse genotypes following oral saline or sucrose administration. Experimental and statistical details are given in the legend of Fig. 3. White bars denote wt; grey, Ctrn-KO; hatched, mGPD-KO; and black, double-KO mice. Data from each group of mice are expressed as mean ± SD. Numbers in parentheses denote the number of mice in each genotype examined.

dehydrogenase reaction would limit the overall conversion of glyceraldehyde-3-phosphate to 1,3-bisphosphoglycerate, and therefore shunt excess glyceraldehyde-3-phosphate from the catabolism of both glucose and fructose towards DHAP via the triose phosphate isomerase reaction. Our results support the notion that DHAP is further converted to G3P, as the cytosolic glycerol-3-phosphate dehydrogenase reaction is driven in the direction of G3P synthesis by the increased cytosolic NADH/NAD^+ ratio. In the case of the double-KO mice, G3P appears to then act as a dead-end metabolite (much like lactate), and simply accumulates. However, as G3P should still be available for fatty acid esterification, it is unclear whether the level of hepatic G3P observed in the double-KO mice represents an altered equilibrium or a rate limitation in triglyceride synthesis. The hypertriglyceridemia observed in citrin-deficient patients is believed to be due to the utilization of the malate–citrate cycle

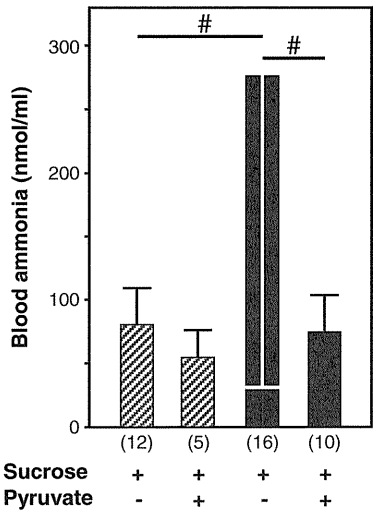

Fig. 8. Effect of oral sodium pyruvate (20 mmol/kg; Na-Pyr) administration on hyperammonemia induced by sucrose (5 g/kg body weight) administration in double-KO mice. A sucrose solution (25%), or sucrose with 1 M Na-Pyr solution, was administered to the mice by gastric tube. One hour after administration, blood was taken by cardiac puncture under anesthesia and blood ammonia levels were determined. Hatched bars denote mGPD-KO littermate controls; black bars denote double-KO mice. Data from each group of mice are expressed as mean ± SD. Differences between each genotype and treatment group were evaluated using a Student's *t*-test, where # denotes a statistical difference at $p<0.05$.

as an alternative for transporting cytosolic NADH into the mitochondria, which would require the transport of citrate out of the mitochondria, and its conversion to acetyl-CoA for fatty acid synthesis. This process is cataplerotic, since citrate, a TCA cycle intermediate, is being utilized. Further studies are needed to examine the relationship between the G3P/DHAP and Lac/Pyr ratios in the double-KO mice, as well as their overall consequences on malonyl-CoA levels and fatty acid biosynthesis in relation to the overall rate of triglyceride biosynthesis.

Inhibition of the glyceraldehyde-3-phosphate dehydrogenase reaction is also hypothesized to limit the amount of pyruvate generated from the catabolism of sucrose, and the increased cytosolic NADH/NAD^+ ratio would convert pyruvate to lactate via lactate dehydrogenase, further limiting its availability for conversion to acetyl-CoA as part of the TCA cycle. The increased hepatic Ala observed in wt and mGPD-KO mice following sucrose versus saline administration was not observed in the Ctrn-KO and double-KO mice, which supports a reduced flow of 3-carbon intermediates through glycolysis. The resulting decreased TCA cycle intermediates citrate, αKG and malate that were found by CE/MS and confirmed using enzymatic methods, further supports the notion that this reduction may lead to decreased ATP synthesis and a possible energy deficit. However, an initial evaluation of hepatic ATP, ADP levels and ATP/ADP ratios in wt, Ctrn-KO, mGPD-KO and double-KO mice, following either saline or sucrose administration, found only decreased ATP levels and ATP/ADP ratios following sucrose administration in all genotypes (data not shown).

If hepatic G3P is acting as a buffer for NADH to normalize the NADH/NAD^+ ratio and mitigating an increased NADH/NAD^+ ratio, what are the cellular consequences of elevated hepatic G3P? Other metabolic disorders that lead to elevated phosphorylated metabolites such as hereditary fructose intolerance (leading to an accumulation of fructose-1-phosphate), classical galactosemia (leading to an accumulation of galactose-1-phosphate) and glycogen storage disease type I (leading to an accumulation of glucose-6-phosphate) all show toxic and damaging cellular effects. One possible mechanism for their toxicity may be

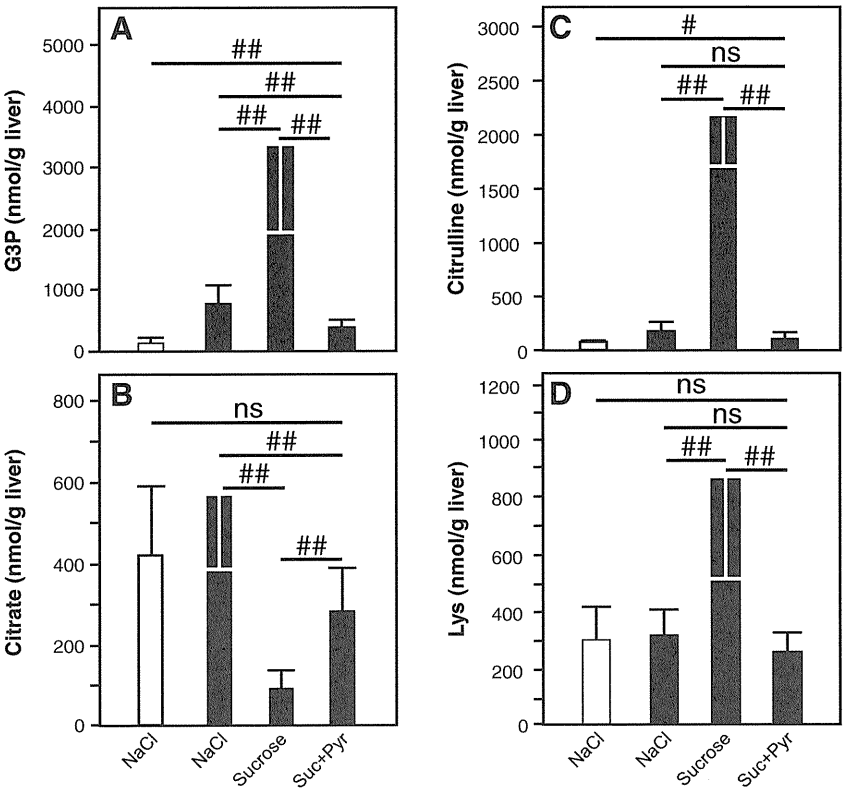

Fig. 9. Hepatic glycerol-3-phosphate (G3P; A), citrate (B), citrulline (C) and lysine (Lys; D) levels in double-KO mice following oral saline (NaCl), sucrose (5 g/kg; Suc) or sucrose with Na-Pyr (20 mmol/kg) administration. Experimental and statistical details are given in the legend of Fig. 8. Livers from the mice were removed and extracted as described in Fig. 3. White bars denote wt mice, for reference; black bars denote double-KO mice. Data from each group of mice are expressed as mean ± SD. The number of mice within each group examined was $n=7$ for wt; $n=8$ for all groups of double-KO mice. Differences between each group of mice were evaluated using a Student's *t*-test, where # denotes a statistical difference at $p<0.05$; ## at $p<0.01$; and ns denotes not statistically different.

through the sequestration of phosphate, decreasing cellular phosphate pools, and limiting energy-dependent pathways. Further work is needed to evaluate the hepatic consequences of an increased hepatic G3P level in the double-KO mice, and whether chronic elevations may lead to carcinogenic conversion, explaining the increased risk of hepatocellular carcinoma in citrin-deficient patients. It is also interesting to note that, similar to the dietary predilections of citrin-deficient patients, peculiar feeding habits with an avoidance of fructose-containing foods are recognized behavior patterns in patients with hereditary fructose intolerance. This behavior has been directly attributed to ingesting fructose which leads to symptoms including poor growth, jaundice, liver steatosis and hypoglycemia [39]— symptoms that overlap those of citrin-deficient patients.

In contrast to the decreased TCA cycle intermediates found in the double-KO mice following sucrose administration, the generalized increase of TCA cycle intermediates found in the Ctrn-KO and double-KO mice following oral saline administration when compared to wt and mGPD-KO mice may be the result of inhibition of gluconeogenesis during the postprandial period. As shown by Moriyama et al. [25], gluconeogenesis from lactate, which is dependent on citrin as the liver-type AGC, is completely inhibited in the perfused livers of Ctrn-KO mice because of its stoichiometric requirement on cytosolic NADH, as predicted by Krebs et al. [22]. The inhibition of gluconeogenesis from lactate, which requires its conversion to pyruvate, translocation into the mitochondria and conversion to oxaloacetate, would potentially trap oxaloacetate (and other TCA cycle intermediates) within the mitochondria as the transport of mitochondrial malate would also be inhibited by an elevated cytosolic NADH/NAD^+ ratio. Additional studies are needed to further investigate this observation.

The substantial increase of hepatic citrulline and decreased Orn in the context of hyperammonemia provides evidence that the argininosuccinate synthetase (ASS) reaction is the rate-limiting or inhibited step of the urea cycle in double-KO mice following sucrose administration. This finding is consistent with what has been observed in CTLN2 patients: the ASS reaction appears specifically sensitive to the loss of citrin function. Contrary to what was found by CE/MS analysis, however, ASA and Arg were found to be elevated in Ctrn-KO and double-KO mice compared to wt and mGPD-KO mice irrespective of oral administration, which may represent elevated steady-state levels in those genotypes. As mitochondrial Asp has been shown to be the preferred source for ASS to condense citrulline and Asp to form ASA [40], cytosolic Asp from either oxaloacetate or asparagine would become essential sources in the absence of citrin. Following sucrose administration that results in an elevated cytosolic NADH/NAD^+ ratio, cytosolic malate dehydrogenase would be inhibited from converting malate to oxaloacetate, further eliminating an essential source of Asp for the ASS reaction via transamination by aspartate aminotransferase. Our previous studies had found increased mRNA expression of asparagine synthetase in the livers of the double-KO mice [27], among other changes, suggesting that asparagine is probably an important source of cytosolic Asp in the double-KO mice despite no observed change in hepatic asparagine levels among the various genotypes or following sucrose administration.

One surprising result from the present metabolome study that appeared seemingly unrelated to the expected roles of citrin in intermediary metabolism, was the finding of a marked increase in hepatic Lys in the double-KO mice after oral sucrose administration. Cross-over point analysis showing the increased Lys (found by CE/MS analysis and confirmed by enzymatic methods) and decreased saccharopine and aminoadipic acid (found by CE/MS analysis) supports a block in Lys oxidation through the inhibition of L-lysine-α-ketoglutarate reductase activity. This was further supported by increased hepatic N^6-acetyl-Lys found by CE/MS analysis; a known byproduct of elevated Lys. L-lysine-α-ketoglutarate reductase [EC.1.5.1.8] activity (one of two enzymatic activities of the bifunctional α-aminoadipate δ-semialdehyde synthase [AASS] enzyme) utilizes NADPH to irreversibly convert lysine and αKG to saccharopine, which is then irreversibly converted to α-aminoadipate δ-semialdehyde by the saccharopine dehydrogenase [EC.1.5.1.9] activity of the same AASS enzyme. Since AASS is a mitochondria matrix enzyme [41], the decreased hepatic αKG found in the double-KO mice following oral sucrose administration (Figs. 1 and 4) may in fact limit the enzymatic conversion of lysine to saccharopine by AASS. A similar secondary hyperlysinemia phenomenon has been observed in several inborn errors of metabolism including urea cycle disorders and pyruvate carboxylase deficiency, where elevated plasma Lys has often been observed. Kamoun et al. [42] have postulated that the elevated plasma Lys levels in those disorders are at least in part dependent on the rate of mitochondrial Lys degradation, and hence the availability of mitochondrial αKG in the liver.

Finally, the identification of these metabolic derangements in double-KO mice following oral sucrose administration has now established additional biomarkers for evaluating the efficacy of candidate therapies in our mouse model of human citrin deficiency. The use of Na-Pyr, which was found previously to be effective in alleviating the block in ureogenesis from ammonium chloride in the perfused liver of Ctrn-KO mice [25], has now been found to lower blood ammonia as well as hepatic G3P, citrulline and Lys levels, and to raise hepatic citrate levels, in double-KO mice following oral sucrose administration. This is in keeping with observations made in a small number of citrin-deficient patients where the administration of Na-Pyr together with Arg has led to increases in body height and weight, normalization of abnormal laboratory findings (e.g., lower plasma citrulline, threonine/serine ratio and serum pancreatic secretory trypsin inhibitor levels), and improvement of the histological appearance of the liver in repeat biopsies [13,43]. Overall, our results support the hypothesis that increased sucrose metabolism in human citrin deficiency alters the cytosolic redox state such that the increased NADH/NAD^+ ratio leads to inhibition of multiple pathways of intermediary metabolism including glycolysis, the TCA cycle, ureogenesis, and even Lys catabolism. These results also provide further rationale for the use of Na-Pyr in citrin-deficient patients, where the increased availability of Pyr to decrease the NADH/NAD^+ ratio as well as potentially provide an anaplerotic substrate for the TCA cycle likely explains its therapeutic effect. We are now testing the response of more than a dozen citrin-deficient patients to Na-Pyr treatment.

Acknowledgments

This study was supported in part by KAKENHI (C 21591337), JSPS Asia Africa Science Platform Program, Adaptable and Seamless Technology Transfer Program through Target-driven R & D (A-STEP) from Japan Science and Technology, and Grant for Child Health and Development from the Ministry of Health, Labor and Welfare in Japan. We thank Dr. Matin Gore for his help editing the manuscript. We also deeply regret that one of the authors, Dr. Keiko Kobayashi, passed away in December, 2010.

References

[1] K. Kobayashi, D.S. Sinasac, M. Iijima, A.P. Boright, L. Begum, J.R. Lee, T. Yasuda, S. Ikeda, R. Hirano, H. Terazono, M.A. Crackower, I. Kondo, L.C. Tsui, S.W. Scherer, T. Saheki, The gene mutated in adult-onset type II citrullinaemia encodes a putative mitochondrial carrier protein, Nat. Genet. 22 (1999) 159–163.

[2] L. Palmieri, B. Pardo, F.M. Lasorsa, A. del Arco, K. Kobayashi, M. Iijima, M.J. Runswick, J.E. Walker, T. Saheki, J. Satrústegui, F. Palmieri, Citrin and aralar1 are Ca (2+)-stimulated aspartate/glutamate transporters in mitochondria, EMBO J. 20 (2001) 5060–5069.

[3] A. del Arco, J. Satrústegui, Molecular cloning of Aralar, a new member of the mitochondrial carrier superfamily that binds calcium and is present in human muscle and brain, J. Biol. Chem. 273 (1998) 23327–23334.

[4] L. Begum, M.A. Jalil, K. Kobayashi, M. Iijima, M.X. Li, T. Yasuda, M. Horiuchi, A. del Arco, J. Satrústegui, T. Saheki, Expression of three mitochondrial solute carriers, citrin, aralar1 and ornithine transporter, in relation to urea cycle in mice, Biochim. Biophys. Acta 1574 (2002) 283–292.

[5] Y. Tazawa, K. Kobayashi, T. Ohura, D. Abukawa, F. Nishinomiya, Y. Hosoda, M. Yamashita, I. Nagata, Y. Kono, T. Yasuda, N. Yamaguchi, T. Saheki, Infantile cholestatic jaundice associated with adult-onset type II citrullinemia, J. Pediatr. 138 (2001) 735–740.

[6] T. Tomomasa, K. Kobayashi, H. Kaneko, H. Shimura, T. Fukusato, M. Tabata, Y. Inoue, S. Ohwada, M. Kasahara, Y. Morishita, M. Kimura, T. Saheki, A. Morikawa, Possible clinical and histologic manifestations of adult-onset type II citrullinemia in early infancy, J. Pediatr. 138 (2001) 741–743.
[7] T. Ohura, K. Kobayashi, Y. Tazawa, I. Nishi, D. Abukawa, O. Sakamoto, K. Iinuma, T. Saheki, Neonatal presentation of adult-onset type II citrullinemia, Hum. Genet. 108 (2001) 87–90.
[8] T. Saheki, K. Kobayashi, Mitochondrial aspartate glutamate carrier (citrin) deficiency as the cause of adult-onset type II citrullinemia (CTLN2) and idiopathic neonatal hepatitis (NICCD), J. Hum. Genet. 47 (2002) 333–341.
[9] K. Kobayashi, T. Saheki, Citrin deficiency, in: R.A. Pagon, T.C. Bird, C.R. Dolan, K. Stephens (Eds.), GeneReviews [Internet], University of Washington, Seattle, Seattle (WA), 1993.
[10] T. Ohura, K. Kobayashi, Y. Tazawa, D. Abukawa, O. Sakamoto, S. Tsuchiya, T. Saheki, Clinical pictures of 75 patients with neonatal intrahepatic cholestasis caused by citrin deficiency (NICCD), J. Inherit. Metab. Dis. 30 (2007) 139–144.
[11] T. Saheki, K. Kobayashi, M. Iijima, M. Moriyama, M. Yazaki, Y. Takei, S. Ikeda, Metabolic derangements in deficiency of citrin, a liver-type mitochondrial aspartate–glutamate carrier, Hepatol. Res. 33 (2005) 181–184.
[12] D. Dimmock, K. Kobayashi, M. Iijima, A. Tabata, L.J. Wong, T. Saheki, B. Lee, F. Scaglia, Citrin deficiency: a novel cause of failure to thrive that responds to a high-protein, low-carbohydrate diet, Pediatrics 119 (2007) e773–e777.
[13] K. Mutoh, K. Kurokawa, K. Kobayashi, T. Saheki, Treatment of a citrin-deficient patient at the early stage of adult-onset type II citrullinaemia with arginine and sodium pyruvate, J. Inherit. Metab. Dis. (2008) [Epub ahead of print].
[14] M. Hachisu, Y. Oda, M. Goto, K. Kobayashi, T. Saheki, T. Ohura, S. Noma, S. Kitanaka, Citrin deficiency presenting with ketotic hypoglycaemia and hepatomegaly in childhood, Eur. J. Pediatr. 164 (2005) 109–110.
[15] Y. Imamura, K. Kobayashi, T. Shibatou, S. Aburada, K. Tahara, O. Kubozono, T. Saheki, Effectiveness of carbohydrate-restricted diet and arginine granules therapy for adult-onset type II citrullinemia: a case report of siblings showing homozygous SLC25A13 mutation with and without the disease, Hepatol. Res. 26 (2003) 68–72.
[16] S. Ikeda, S. Kawa, Y. Takei, K. Yamamoto, H. Shimojo, K. Tabata, K. Kobayashi, T. Saheki, Chronic pancreatitis associated with adult-onset type II citrullinemia: clinical and pathologic findings, Ann. Intern. Med. 141 (2004) W109–W110.
[17] M. Komatsu, M. Yazaki, N. Tanaka, K. Sano, E. Hashimoto, Y. Takei, Y.Z. Song, E. Tanaka, K. Kiyosawa, T. Saheki, T. Aoyama, K. Kobayashi, Citrin deficiency as a cause of chronic liver disorder mimicking non-alcoholic fatty liver disease, J. Hepatol. 49 (2008) 810–820.
[18] N. Hagiwara, Y. Sekijima, Y. Takei, S. Ikeda, S. Kawasaki, K. Kobayashi, T. Saheki, Hepatocellular carcinoma in a case of adult-onset type II citrullinemia, Intern. Med. 42 (2003) 978–982.
[19] C.W. Tsai, C.C. Yang, H.L. Chen, W.L. Hwu, M.Z. Wu, K.L. Liu, M.S. Wu, Homozygous SLC25A13 mutation in a Taiwanese patient with adult-onset citrullinemia complicated with steatosis and hepatocellular carcinoma, J. Formos. Med. Assoc. 105 (2006) 852–856.
[20] Y.Z. Song, B.X. Li, F.P. Chen, S.R. Liu, J.S. Sheng, M. Ushikai, C.H. Zhang, T. Zhang, Z.N. Wang, K. Kobayashi, T. Saheki, X.Y. Zheng, Neonatal intrahepatic cholestasis caused by citrin deficiency: clinical and laboratory investigation of 13 subjects in mainland of China, Dig. Liver Dis. 41 (2009) 683–689.
[21] Y.Z. Song, M. Deng, F.P. Chen, F. Wen, L. Guo, S.L. Cao, J. Gong, H. Xu, G.Y. Jiang, L. Zhong, K. Kobayashi, T. Saheki, Z.N. Wang, Genotypic and phenotypic features of citrin deficiency: five-year experience in a Chinese pediatric center, Int. J. Mol. Med. 28 (2011) 33–40.
[22] H.A. Krebs, T. Gascoyne, B.M. Notton, Generation of extramitochondria reducing power in gluconeogenesis, Biochem. J. 102 (1967) 275–282.
[23] T. Saheki, K. Kobayashi, M. Terashi, T. Ohura, Y. Yanagawa, Y. Okano, T. Hattori, H. Fujimoto, K. Mutoh, Z. Kizaki, A. Inui, Reduced carbohydrate intake in citrin-deficient subjects, J. Inherit. Metab. Dis. 31 (2008) 386–394.
[24] D.S. Sinasac, M. Moriyama, M.A. Jalil, L. Begum, M.X. Li, M. Iijima, M. Horiuchi, B.H. Robinson, K. Kobayashi, T. Saheki, L.C. Tsui, Slc25a13-knockout mice harbor metabolic deficits but fail to display hallmarks of adult-onset type II citrullinemia, Mol. Cell. Biol. 24 (2004) 527–536.
[25] M. Moriyama, M.X. Li, K. Kobayashi, D.S. Sinasac, Y. Kannan, M. Iijima, M. Horiuchi, L. C. Tsui, M. Tanaka, Y. Nakamura, T. Saheki, Pyruvate ameliorates the defect in ureogenesis from ammonia in citrin-deficient mice, J. Hepatol. 44 (2006) 930–938.
[26] D. Sadava, M. Depper, M. Gilbert, B. Bernard, E.R. McCabe, Development of enzymes of glycerol metabolism in human fetal liver, Biol. Neonate 52 (1987) 26–32.
[27] T. Saheki, M. Iijima, M.X. Li, K. Kobayashi, M. Horiuchi, M. Ushikai, F. Okumura, X.J. Meng, I. Inoue, A. Tajima, M. Moriyama, K. Eto, T. Kadowaki, D.S. Sinasac, L.C. Tsui, M. Tsuji, A. Okano, T. Kobayashi, Citrin/mitochondrial glycerol-3-phosphate dehydrogenase double knock-out mice recapitulate features of human citrin deficiency, J. Biol. Chem. 282 (2007) 25041–25052.
[28] K. Eto, Y. Tsubamoto, Y. Terauchi, T. Sugiyama, T. Kishimoto, N. Takahashi, N. Yamauchi, N. Kubota, S. Murayama, T. Aizawa, Y. Akanuma, S. Aizawa, H. Kasai, Y. Yazaki, T. Kadowaki, Role of NADH shuttle system in glucose-induced activation of mitochondrial metabolism and insulin secretion, Science 283 (1999) 981–985.
[29] T. Kuhara, Diagnosis of inborn errors of metabolism using filter paper urine, urease treatment, isotope dilution and gas chromatography-mass spectrometry, J. Chromatogr. B Biomed. Sci. 758 (2001) 3–25.
[30] T. Kuhara, Noninvasive human metabolome analysis for differential diagnosis of inborn errors of metabolism, J. Chromatogr. B 855 (2007) 42–50.
[31] T. Soga, R. Baran, M. Suematsu, Y. Ueno, S. Ikeda, T. Sakurakawa, Y. Kakazu, T. Ishikawa, M. Robert, T. Nishioka, M. Tomita, Differential metabolomics reveals ophthalmic acid as an oxidative stress biomarker indicating hepatic glutathione consumption, J. Biol. Chem. 281 (2006) 16768–16776.
[32] G. Lang, L(−)-Glycerol 3-phosphate, in: H.U. Bergmeyer, J. Bergmeyer, M. Grassl (Eds.), third ed., Methods of Enzymatic Analysis, Vol. VI, Verlag Chemie, Weinheim, 1984, pp. 525–531.
[33] G. Michal, D-Fructose 1,6-bisphosphate, Dihydroxyacetone phosphate and D-glycealdehyde 3-phosphate, in: H.U. Bergmeyer, J. Bergmeyer, M. Grassl (Eds.), third ed., Methods of Enzymatic Analysis, Vol. VI, Verlag Chemie, Weinheim, 1984, pp. 342–350.
[34] W. Lamprecht, F. Heinz, Pyruvate, in: H.U. Bergmeyer, J. Bergmeyer, M. Grassl (Eds.), third ed., Methods of Enzymatic Analysis, Vol. VI, Verlag Chemie, Weinheim, 1984, pp. 570–577.
[35] H. M llering, Citrate, in: H.U. Bergmeyer, J. Bergmeyer, M. Graßl (Eds.), third ed., Methods of Enzymatic Analysis, Vol. VII, VCH Verlagsgesellschaft, Weinheim, 1985, pp. 2–12.
[36] H. Möllering, L-(−)-Malate, Determination with Malate Dehydrogenase and Aspartate Aminotransferase, in: H.U. Bergmeyer, J. Bergmeyer, M. Graßl (Eds.), third ed., Methods of Enzymatic Analysis, Vol. VII, VCH Verlagsgesellschaft, Weinheim, 1985, pp. 39–47.
[37] A. Burlina, 2-Oxoglutarate, in: H.U. Bergmeyer, J. Bergmeyer, M. Graßl (Eds.), third ed., Methods of Enzymatic Analysis, Vol. VII, VCH Verlagsgesellschaft, Weinheim, 1985, pp. 20–24.
[38] P. Husek, Chloroformate in gas chromatography as general purpose derivatizing agents, J. Chromatogr. B Biomed. Sci. Appl. 717 (1998) 57–91.
[39] R. Gitzelmann, B. Steinmann, G. Van den Berghe, Disorders of Fructose Metabolism, in: C.R. Scriver, A.L. Beaudet, W.S. Sly, D. Valle (Eds.), seventh ed., The Metabolic and Molecular Bases of Inherited Disease, Vol. I, 1995, pp. 905–934.
[40] A.J. Meijer, J.A. Gimpel, G. Deleeuw, M.E. Tischler, J.M. Tager, J.R. Williamson, Interrelationships between gluconeogenesis and ureogenesis in isolated hepatocytes, J. Biol. Chem. 253 (1978) 2308–2320.
[41] K.P. Blemings, T.D. Crenshaw, R.W. Swick, N.J. Benevenga, Lysine-alpha-ketoglutarate reductase and saccharopine dehydrogenase are located only in the mitochondrial matrix in rat liver, J. Nutr. 124 (1994) 1215–1221.
[42] P. Kamoun, V. Richard, D. Rabier, J.M. Saudubray, Plasma lysine concentration and availability of 2-ketoglutarate in liver mitochondria, J. Inherit. Metab. Dis. 25 (2002) 1–6.
[43] T. Saheki, K. Inoue, A. Tushima, K. Mutoh, K. Kobayashi, Citrin deficiency and current treatment concepts, Mol. Genet. Metab. 100 (2010) S59–S64.

Molecular Genetics and Metabolism 102 (2011) 349–355

Contents lists available at ScienceDirect

Molecular Genetics and Metabolism

journal homepage: www.elsevier.com/locate/ymgme

Induction of PDK4 in the heart muscle of JVS mice, an animal model of systemic carnitine deficiency, does not appear to reduce glucose utilization by the heart

Miharu Ushikai [a,b,1], Masahisa Horiuchi [c,*,1], Keiko Kobayashi [a], Sadayuki Matuda [d], Akio Inui [b], Toru Takeuchi [c], Takeyori Saheki [a,e]

[a] Department of Molecular Metabolism and Biochemical Genetics, Kagoshima University Graduate School of Medical and Dental Sciences, Kagoshima 890-8544, Japan
[b] Department of Psychosomatic Internal Medicine, Kagoshima University Graduate School of Medical and Dental Sciences, Kagoshima 890-8544, Japan
[c] Department of Environmental Medicine, Kagoshima University Graduate School of Medical and Dental Sciences, Kagoshima 890-8544, Japan
[d] Department of Health Science, National Institute of Fitness and Sports in Kanoya, Kanoya 891-2393, Japan
[e] Institute for Health Sciences, Tokushima Bunri University, Tokushima 770-8514, Japan

ARTICLE INFO

Article history:
Received 24 November 2010
Accepted 25 November 2010
Available online 9 December 2010

Keywords:
Cardiac hypertrophy
Carnitine deficiency
Glucose uptake
Juvenile visceral steatosis (JVS) mice
Pyruvate dehydrogenase complex

ABSTRACT

Pyruvate dehydrogenase kinase 4 (PDK4) mRNA has been reported as an up-regulated gene in the heart and skeletal muscle of carnitine-deficient juvenile visceral steatosis (JVS) mice under fed conditions. PDK4 plays an important role in the inhibition of glucose oxidation via the phosphorylation of pyruvate dehydrogenase complex (PDC). This study evaluated the meaning of increased PDK4 mRNA in glucose metabolism by investigating PDK4 protein levels, PDC activity and glucose uptake by the heart and skeletal muscle of JVS mice. PDK4 protein levels in the heart and skeletal muscle of fed JVS mice were increased in accordance with mRNA levels, and protein was enriched in the mitochondria. PDK4 protein was co-fractionated with PDC in sucrose density gradient centrifugation, like PDK2 protein; however, the activities of the pyruvate dehydrogenase complex (PDC) active form in the heart and skeletal muscle of fed JVS mice were similar to those in fed control mice. Fed JVS mice showed significantly higher glucose uptake in the heart and similar uptake in the skeletal muscle compared with fed control mice. Thus, in carnitine deficiency under fed conditions, glucose was preferentially utilized in the heart as an energy source despite increased PDK4 protein levels in the mitochondria. The preferred glucose utilization may be involved in developing cardiac hypertrophy from carnitine deficiency in fatty acid oxidation abnormality.

1. Introduction

Juvenile visceral steatosis (JVS) mice, an animal model of systemic carnitine deficiency (SCD), showed cardiac hypertrophy and progressive cardiac dysfunction [1–6]. In SCD, heart problems including hypertrophy and arrhythmia are clinically important [7,8]. Understanding the pathophysiology of the hypertrophy of JVS mice will help to prevent and treat heart problems in human SCD. Here, we tried to study the pathophysiology of hypertrophy by elucidating the role of pyruvate dehydrogenase kinase (PDK) 4, which was found as an up-regulated gene in the hypertrophied heart [9], in glucose metabolism.

JVS mice were discovered originally in the C3H•OH strain suffering from fatty liver [10]. Subsequent studies revealed that JVS mice also have hypoglycemia, hyperammonemia, growth retardation and cardiac hypertrophy, in addition to fatty liver, thus resembling the symptoms of human SCD [3,11]. JVS mice showed severely lowered carnitine levels in blood due to lowered renal reabsorption of carnitine [12,13]. Genetically, JVS mice showed a spontaneous mutation in the mouse homologue of organic cation transporter 2 (OCTN2), as well as human SCD [14,15]. Thus, JVS mice are now established as an animal model for human SCD. Cardiac hypertrophy was ameliorated by intraperitoneal administration of carnitine. Additionally, peroxisome proliferator-activated receptor alpha (PPARα) agonists [16], or lowering the fat content of the diet [17] attenuated hypertrophy, suggesting that fatty acids which cannot be metabolized are involved in its development. Antioxidants are also effective, indicating that oxidative stress plays an important role in hypertrophy [18]; however, the mechanism of hypertrophy is still not

Abbreviations: BCKDC, branched-chain ketoacid dehydrogenase complex; DTT, dithiothreitol; E1, pyruvate dehydrogenase component of PDC; E2, dihydrolipoyl acetyltransferase component of PDC; E3, dihydrolipoamide dehydrogenase component of PDC; E3BP, E3-binding protein component of PDC; HA, hemagglutinin antigen; JVS, juvenile visceral steatosis; KGDC, α-ketoglutarate dehydrogenase complex; LDH, lactate dehydrogenase; PDC, pyruvate dehydrogenase complex; PDK, pyruvate dehydrogenase kinase.

* Corresponding author. Kagoshima University Graduate School of Medical and Dental Sciences, 8-35-1 Sakuragaoka, Kagoshima 890-8544, Japan. Fax: +81 99 265 8434.
E-mail address: masakun@m.kufm.kagoshima-u.ac.jp (M. Horiuchi).

[1] These two authors contributed equally to this study.

1096-7192/$ – see front matter © 2010 Elsevier Inc. All rights reserved.
doi:10.1016/j.ymgme.2010.11.167

completely understood. For better understanding, differences in gene expressions between hypertrophied and normal hearts were surveyed. JVS mice showed mRNA of atrial natriuretic peptide and skeletal muscle actin up-regulated in the heart as well as the pressure-overloaded hypertrophied heart [4]. On the other hand, JVS mice showed unchanged mRNA in β-myosin heavy chain and decreased mRNA in cardiotrophin [4,19], different from the pressure-overloaded hypertrophied heart. These results indicate that the mechanism of hypertrophy is at least partially different from that of pressure-overloaded hypertrophy. We also found that pyruvate dehydrogenase kinase (PDK) 4 mRNA, which has been reported as a down-regulated gene in the pressure-overloaded hypertrophied heart, was increased in the heart of JVS mice [9,20,21]. As noted in studies on pressure-overloaded hypertrophy, down-regulated PDK4 is involved in the increased reliance on glucose as fuel [20]. It is interesting to examine whether increased PDK4 mRNA in the JVS mice heart plays a role in glucose metabolism through pyruvate dehydrogenase complex (PDC) regulation.

PDK isoforms have been reported as four respective proteins, which are coded to four different genes. The four PDK isoforms are shown on tissue distribution, affinity to substrates, and sensitivity to inhibitors [22]. All PDK isoforms are considered to be involved in the inactivation of PDC. PDK4 has been proposed to be especially involved in PDC inactivation under fasting or diabetic conditions through transcriptional regulation [23–26]. The physical association between PDK4 and PDC has not been elucidated completely, but the remaining PDK isoforms (PDK1-3) have been shown to bind to PDC through the E2-lipoyl domain [27–29]. Recently, Wynn et al. reported that PDK4 possibly binds to PDC through the E3BP-lipoyl domain [30]. It is necessary to show clearly the physical binding between PDK4 and PDC. In JVS mice, the activity of the PDC active form (PDCa) in the heart of carnitine-deficient mice was similar to that in control mice [9], suggesting that the increased PDK4 mRNA level is not necessarily associated with PDC inactivation.

In the present study, we examined the relationship between PDK4 protein levels and PDC activity in the heart and skeletal muscles of JVS mice. We also observed the localization of PDK4 protein in JVS mice and the physical association between PDK4 and PDC. Glucose uptake was also measured in several JVS mouse tissues.

2. Methods

2.1. Animals and reagents

Control (W, $jvs^{+/+}$) and homozygous mutant (JVS, $jvs^{-/-}$) mice were obtained by cross-mating heterozygous mice or by mating homozygous mutant male and heterozygous female mice [10]. Mice residing in a closed colony originating from the C3H•OH strain were used for all experiments. Neonatal (7–28 days of age) JVS mice were treated intraperitoneally with L-carnitine·HCl (5 μmol/mouse; Sigma-Aldrich, St. Louis, MO), dissolved in physiological saline and neutralized with 0.2 M NaOH, as described previously [31]. Mice were kept under a 12 h lights on–off cycle (lights on 7:00–19:00) and had free access to laboratory chow (CE2; CLEA Japan, Inc., Tokyo, Japan) and water.

This study was approved by the Ethics Committee for Animal Experimentation at Kagoshima University, which was standardized to Japanese national guidelines for animal experiments.

Except when noted, reagents were purchased from Nacalai Tesque (Kyoto, Japan) and Sigma-Aldrich. Anti-hemagglutinin (HA) antibody and peroxidase conjugated secondary antibodies were from Santa Cruz Biotechnology (Santa Cruz, CA) and Roche Diagnostics (Tokyo, Japan), respectively.

2.2. Preparation of antibodies, and Western blotting

Anti-PDK4 antibody (αPDK4) antigen was prepared as follows. The PCR product of PDK4 from mouse heart cDNA was introduced into pET-15b expression vector (Novagen, Madison, MI) to produce His_6-tagged protein. Primers (forward primer, 5′-ATCATATGAAGCAGCTGCTG-GACTTTG-3′; reverse primer, 5′-AGACCCACTTGGATCCCGTAAA-3′) were utilized for PCR. These contained mismatched sequences to produce *Nde*I and *BamH*I restriction enzyme sites (underlined). Plasmids containing the PCR product were transformed in BL21 (DE3) pLysS cells. The purified protein was mixed with TiterMax Gold (CytRx, Norcross, GA) in accordance with the manufacturer's protocol, and injected into a rabbit. This gave serum reacting specifically against recombinant mouse PDK4 proteins (Fig. 2A).

Anti-PDK2 antibody (Drs. P. Wu and R.A. Harris, Indiana University, IN) [24], and anti-branched chain α-ketoacid dehydrogenase complex (BCKDC) antibody (Dr. Y. Shimomura, Nagoya Institute of Technology, Japan) [32] were kindly donated. Anti-PDC and anti-α-ketoglutarate dehydrogenase complex (KGDC) antibodies were prepared [33].

Mouse PDK1, PDK2 and PDK4 proteins containing a hemagglutinin (HA) tag at the carboxyl-terminal region were produced. The cDNA clones for mouse PDK1 (register number, IMAGp998K234710Q2) and PDK2 (register number, IMAGp998N044710Q2) were obtained from RZPD Deutsches Ressourcenzentrum (Berlin, Germany). The cDNA clone for PDK4 was prepared from a mouse heart cDNA [9]. PCR products (PDK1, 5′-GACCATGAGGCTGGCAAGGCTG-3′ and 5′-GCTCGAGTTAAGCGTAGTCTG- GGACGTCGTATGGGTAAGAGCTTCG-GAATGTGGT-3′; PDK2, 5′-GACCATGCGT- TGGGTCCGGGC-3′ and 5′-GCTCGAGCTAAGCGTAGTCTGGGACGTCGTATGGGT- AGCTGACCCGA-3′; PDK4, 5′-GACCATGAAGGCAGCCCGCTTC-3′ and 5′-GCTCGAGTCAAGCG-TAGTCTGGGACGTCGTATGGGTACACTGCCAGCTTCTCCTTC-3′) were subcloned into a eukaryotic expression vector, pcDNA3.1 (Invitrogen, Carlsbad, CA). The underlined portions of the primers mentioned previously each correspond to a region of the HA tag. The plasmids were transfected into COS cells by the calcium-phosphate method [34]. The recombinant proteins were homogenized by buffer A (137 mM NaCl, 2.7 mM KCl, 10 mM Na_2HPO_4, 1.8 mM KH_2PO_4, pH 7.4).

For Western blot analysis, samples were treated with an equal volume of SDS buffer [0.12 M Tris–HCl pH 6.8, 2% (w/v) SDS, 20% (v/v) glycerol, and 0.4% (w/v) bromphenol blue, 200 mM DTT]. Electrophoresis (10% SDS-PAGE) and transfer followed the manufacturer's instructions (Bio-Rad, Hercules, CA). Nitrocellulose membrane was purchased from Bio-Rad. An ECL kit (PIERCE, Rockford, IL) was used to detect immunoreactive materials. The detected signals were quantified by ChemiDoc XRS and Quantity One software (Bio-Rad).

2.3. Real-time PCR for quantification of PDK2, PDK4 and PDP1mRNAs

Total RNA was isolated from anesthetized mice (pentobarbital: 100 mg/kg body weight) using the method of Chomczynski and Sacchi [35]. Isolated RNA was treated with DNAase (Ambion Inc., Austin, TX) to delete genomic contamination. First-strand cDNA was synthesized using 5 μg total RNA and oligo-$(dT)_{12-18}$ primer following the manufacturer's instructions (Invitrogen). Real-time quantitative PCR was performed using SYBR-Green on a Thermal Cycler Dice Real Time System (Takara Bio Inc., Otsu, Japan). The cyclophylin gene was used as an internal control for all samples. The cycle threshold number (Ct) at which amplification entered the exponential phase was determined for each gene under investigation. Gene expression levels were analyzed using the delta-delta Ct method, determining the target gene expression relative to an internal control and relative to control individual samples. The primers used were as follows: 5′-CAGCGTGTCTGATGTGGTGA-3′ and 5′-CAGGTCAGGGGAAGCCATG-3′ for PDK2 [36]; 5′-TTTGGTGGAGTTCCATGAGAA-3′ and 5′-GAACTTT-GACCAGCGTGTCT-3′ for PDK4 [9]; 5′-ACTGGTATGCATCACCAACAG-3′ and 5′-ACACTGATGACATCTTTGCTCT-3′ for pyruvate dehydrogenase phosphatase catalytic subunit 1 (PDP1) (NM_001033453) [37]; 5′-GGTGGAGAGCACCAAGACAGA-3′ and 5′-GCCGGAGTCGACAATGATG-3′ for cyclophilin [38].

2.4. Measurement of PDC activity of active and total forms [39,40]

For the active form, hearts and skeletal muscles were taken from anesthetized mice and immediately freeze-clamped with Wolleneberger tongs pre-cooled in liquid nitrogen. The frozen tissues were homogenized with buffer B (0.25 M sucrose, 5 mM Tris–HCl and 2 mM EGTA, pH 7.4, containing 50 mM sodium fluoride and 10 mM sodium dichloroacetate).

For the total form, fresh tissues were disrupted with a polytron homogenizer in buffer B. Mitochondria were prepared by differential centrifugation and then incubated (30 min at 30 °C) in buffer C (120 mM KCl, 20 mM Tris–HCl, 5 mM potassium phosphate, 2 mM EDTA, pH 7.4) containing 10 mM carbonyl cyanide m-chlorophenylhydrazone, a respiratory inhibitor. The incubated mitochondria were precipitated by centrifugation and frozen at −80 °C. The mitochondria were then thawed (30 °C) with buffer D (50 mM potassium phosphate, 2 mM EGTA, pH 7.0) containing 1.0% (v/v) Triton X-100. Both forms of PDC activities were measured by determining $^{14}CO_2$ production from [1-^{14}C]-pyruvate [39]. Citrate synthase activity [41] was determined spectrophotometrically as an indication of mitochondrial recovery. The unit of PDC activity is defined as 1 μmol substrate converted into product per min at 37 °C. Total PDC activity was calculated as: [PDC activity in mitochondria fraction/citrate synthase activity (mitochondria fraction)] x [citrate synthase activity (homogenate fraction)/mg protein of tissue] [40].

2.5. Tissue homogenization and mitochondria isolation

Tissues from anesthetized mice were taken and frozen until use. The tissues were homogenized by buffer E [30 mM HEPES, 1 mM EDTA, 0.15 M KCl, 3 mM DTT, 0.1% (v/v) Triton X-100, 1 μg/ml pepstatin, 10 μg/ml leupeptin, 0.1 mg/ml pefablock, pH 7.4] with a Potter–Elvehjem homogenizer. For mitochondria isolation, fresh hearts from anesthetized mice were homogenized with buffer F (0.25 M sucrose and 10 mM Tris–HCl, pH7.4). The homogenate was filtrated (75 μm mesh) and centrifuged at 600 ×*g* for 10 min at 4 °C. The supernatant was centrifuged again at 8000 ×*g* for 10 min at 4 °C. The precipitate suspended in buffer E was fractionated to obtain the mitochondrial fraction with a sucrose gradient (1.10–1.56 M sucrose in 10 mM Tris–HCl, pH 7.4) at 82,000 ×*g* for 200 min at 4 °C. Mitochondria fractionation was evaluated by measuring the activities of lactate dehydrogenase (commercial kit; Wako Pure Chemical Industries, Japan) and citrate synthase [41].

2.6. Fractionation of α-ketoacid dehydrogenase complexes with sucrose gradient techniques

The frozen hearts were homogenized with buffer A. The homogenate (Ho) was centrifuged at 600 ×*g* for 10 min at 4 °C, and the supernatant (S1) was centrifuged at 20,000 ×*g* for 10 min at 4 °C to obtain the supernatant (S2) and the precipitate (P2). The precipitate (P2) was suspended in buffer G [30 mM HEPES, 1 mM EDTA, 0.15 M KCl, 3 mM DTT, 0.1% (v/v) Triton X-100]. The suspension was ultra-centrifuged at 100,000 ×*g* for 90 min at 4 °C, and divided into supernatant (S3) and precipitate (P3). This precipitate (P3) was suspended in buffer G and ultra-centrifuged at 100,000 ×*g* for 60 min. This precipitate was designated P4.

The P4 fraction was suspended in buffer G without Triton X-100, and was applied to the top of a sucrose gradient cushion. The sucrose gradient was composed of 4 ml of 1.46 M sucrose and 34 ml of 0.29–0.88 M sucrose in buffer G without Triton X-100. After ultra-centrifugation (50,000 ×*g* for 15 h), 10 drops (about 1.1 ml) were collected from the bottom for fractionation.

2.7. 2-Deoxy-glucose uptake [42–44]

2-Deoxy-glucose uptake was analyzed in tissues using intraperitoneal injections of 2 μCi ([1-^{3}H]2-deoxy-D-glucose)/20 g body weight. The isotope, [1-^{3}H]2-deoxy-glucose ([^{3}H]2-DG; 3 Ci/mmol, 1.0 mCi/ml; Moravek Biochemicals, CA), was diluted with 50 times volume (100 μl) of 0.9% NaCl. Mice were killed by decapitation 30 min after injection. The heart, femoral skeletal muscle, epididymal fat, liver and brain were immediately excised, weighed and homogenized with 6% (w/v) $HClO_4$ in 80 mM triethanolamine. The homogenates were centrifuged at 12,000 ×*g* for 5 min. ^{3}H radioactivity levels of the supernatant from these tissues were measured using a liquid scintillator (Aquasol 2; Perkin Elmer Japan, Japan). Plasma glucose was measured with a commercial kit (Glucose CII-test; Wako, Japan).

2.8. Statistical analysis

Values are shown as the means ± standard deviation (SD). Data were analyzed by unpaired Student's t test. $P<0.05$ was considered significant.

3. Results

3.1. PDK4 mRNA and protein levels in fed and 24 h-fasting JVS mice

To determine PDK4 mRNA and protein levels in fed and fasting JVS adult mice (2–3 months of age), we performed real-time PCR and Western blot (Figs. 1 and 2). Under fed conditions, JVS mice showed significantly higher levels of PDK4 mRNA in the heart than controls, but there were no significant differences in PDK2 mRNA levels between control and JVS mice (Fig. 1). Control mice showed significantly higher levels of PDK4 mRNA in the heart under fasting than fed conditions. JVS mice showed no significant differences in PDK4 mRNA levels of hearts between fed and fasting conditions. Messenger RNA of PDP1, another regulator of PDC, was significantly lower in fed JVS mice than in fed control mice (Fig. 1). PDK4 and PDK2 protein levels were detected by the respective antibodies (Fig. 2). JVS mice under fed conditions showed significantly higher levels of PDK4 protein in the heart, skeletal muscle, liver and kidney than control mice (Fig. 2B). No PDK4 proteins were detected in the brain of either JVS or control mice in this analysis. On the other hand, in fed control mice, PDK2 protein was detected, mainly in the heart, but also faintly in the skeletal muscle, liver, kidney and brain. As shown in Fig. 2C, we compared PDK4 and PDK2 protein levels under fed and fasting conditions. PDK4 protein levels in the hearts of fed JVS mice were significantly higher than in fed control mice, and were not significantly different from 24 h-fasting control mice (Fig. 2C). After

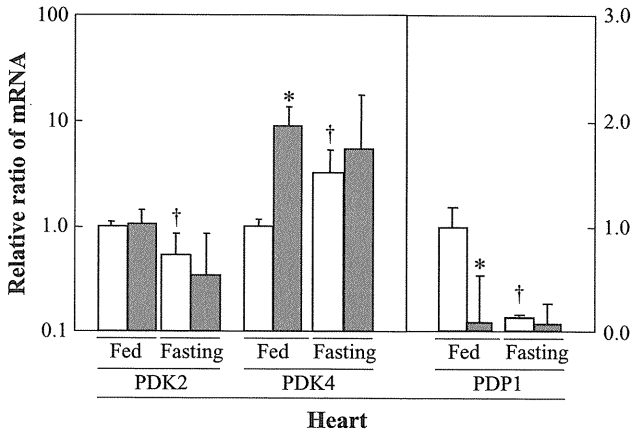

Fig. 1. Quantitative real-time PCR analysis of PDK2, PDK4 and PDP1 in hearts of JVS (gray column) and control (open column) mice under fed and fasting conditions. Gene expression ratios were determined by real-time PCR. The relative values to cyclophilin of fed control mice are set at 1.0. The number of mice used was 4 for each experiment. Values are shown as the means + SD. * denotes $P<0.05$ versus control mice under the respective feeding conditions. †denotes $P<0.05$ versus the respective fed mice.

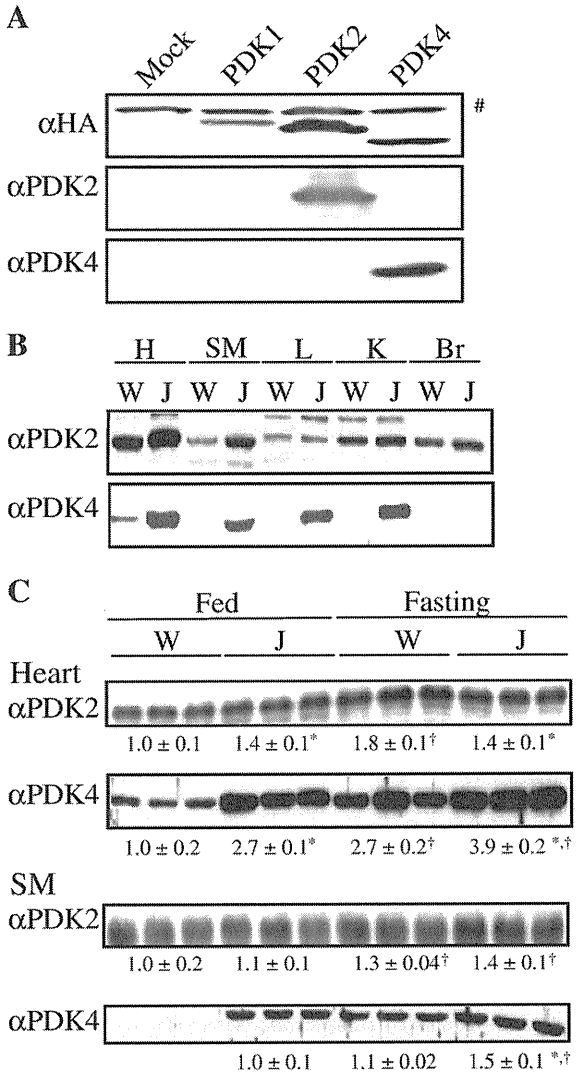

Fig. 2. Western blot analysis. (A) Specificity of the antibodies (αPDK2 and αPDK4) was shown using homogenates (10 μg protein) from COS cells expressing recombinant HA-tagged PDK1, 2 and 4 proteins. "Mock" denotes homogenate from cells transfected with an empty insert vector (pcDNA 3.1). Anti-HA antibody (αHA) detects recombinant proteins and non-specific signals (#). (B) Levels of PDK2 and PDK4 proteins in various organs, including the heart (H), skeletal muscle (SM), liver (L), kidney (K) and brain (Br), of control (W) and JVS (J) mice under fed conditions. Ten μg protein was loaded in each lane. (C) Levels of PDK2 and PDK4 proteins in the heart and skeletal muscle (SM) of control (W) and JVS (J) mice under fed and fasting (24 h) conditions. Quantitative data are shown as the means ± SD. Fed control mice values are set at 1.0 except PDK4 in skeletal muscle. For PDK4 in skeletal muscle, the fed JVS mouse value is set at 1.0. * denotes $P<0.05$ versus control mice under the respective feeding conditions. †denotes $P<0.05$ versus the respective fed mice.

24 h fasting, both JVS and control mice showed a significant increase in PDK4 protein in the heart compared with the respective fed mice. In skeletal muscle, fed JVS mice showed remarkably higher PDK4 protein levels than fed control mice, which had undetectable levels (Fig. 2C). Skeletal muscle PDK4 protein levels in fed JVS mice were not significantly different from those of 24 h-fasting control mice.

3.2. PDC activity of fed and 24 h-fasting JVS mice

We measured the activities of the PDC active form (PDCa) and total PDC (PDCt) in the heart and skeletal muscle. As shown in Table 1, PDCa activities in the heart and skeletal muscle of JVS mice were not significantly different from those of fed control mice. Fed JVS mice showed significantly lower PDCt activity in the heart than fed control mice. After 24 h fasting, PDCa activity significantly decreased in the heart and skeletal muscle of JVS and control mice. Heart PDCt activity in 24 h-fasting control mice was significantly lower than in fed control mice.

3.3. Cellular distribution and physical association with PDC of PDK4 protein

To know why increased PDK4 protein in JVS mice does not contribute to PDC inactivity in the heart and skeletal muscle, we performed experiments and investigated: 1) whether increased PDK4 protein is enriched in the mitochondria of JVS mice, and 2) whether PDK4 protein is physically associated with PDC.

To resolve the first question, we purified mitochondria from the hearts of fed JVS and control mice using ultra-centrifugation and a sucrose gradient (Fig. 3A). The mitochondria fraction showed low contamination of cytosolic components because of very little LDH activity, a cytosolic protein (Fig. 3A). PDK4 protein was enriched in the mitochondrial fraction of control and JVS mice, indicating that increased PDK4 protein was transported in mitochondria. For the second question, PDK4 protein from the heart of fed JVS mice was precipitated after 100,000 ×*g* centrifugation (as with PDK2 and PDC proteins) (Fig. 3B). To examine whether PDK4 protein is bound to PDC, we further fractionated the 100,000 ×*g* precipitate through sucrose density gradient centrifugation. PDK4 protein showed a similar profile to that of PDK2 in the sucrose density gradient (Fig. 3C). PDK2 and PDK4 appeared to be eluted in fractions showing PDC, but not in fractions showing KGDC and BCKDC (Fig. 3C).

3.4. 2-DG uptake

There were no significant differences in plasma glucose between fed control and JVS mice (161 ± 16 versus 165 ± 9 mg/dl, $n = 6$, respectively). 2-DG uptake was measured in control and JVS mice under fed conditions (Fig. 4). JVS mice showed significantly larger 2-DG uptake in the heart and liver than control mice. There were no significant differences in 2-DG uptake in the brain, white adipose tissue and skeletal muscle between control and JVS mice.

4. Discussion

The present study revealed that PDK4 protein, as well as its mRNA level, was increased in the heart and skeletal muscle of carnitine-deficient mice under fed conditions compared with control mice (Figs. 1 and 2). Moreover, PDP1 mRNA, a regulator involved in activation of PDC through its dephosphorylation, was significantly lower in fed JVS mice than in fed control mice (Fig. 1)[37]. On the other hand, there were no significant differences in PDCa activity in the heart and skeletal muscle between control and JVS mice (Table 1). These results suggest that PDK4 is not directly involved in PDC regulation under fed conditions in carnitine deficiency. Also, PDP1 may not play a role in maintaining the activity of

Table 1
PDC active form and total activities under fed and fasting conditions.

	Fed		Fasting (24 h)	
	Active	Total	Active	Total
(mU/mg protein)				
Heart				
W	9.8 ± 4.1 (4)	89.9 ± 7.8 (4)	0.5 ± 0.2[a] (4)	60.0 ± 7.4[a] (4)
JVS	6.3 ± 2.6 (4)	55.2 ± 9.2[b] (4)	1.6 ± 0.6 [a,b](4)	48.7 ± 11.4 (4)
Skeletal muscle				
W	10.9 ± 4.5 (6)	12.5 ± 2.0 (4)	3.6 ± 0.7[a] (6)	16.2 ± 5.1 (4)
JVS	11.5 ± 2.9 (4)	13.1 ± 4.4 (4)	2.3 ± 1.2[a] (4)	16.5 ± 8.2 (4)

The number of mice used is shown in parentheses. Values mean mU of PDC activity over mg of total protein. Values are shown as the means ± SD.
[a] Denotes $P<0.05$ versus the respective fed mice.
[b] Denotes $P<0.05$ versus control mice (W) under the respective feeding conditions.

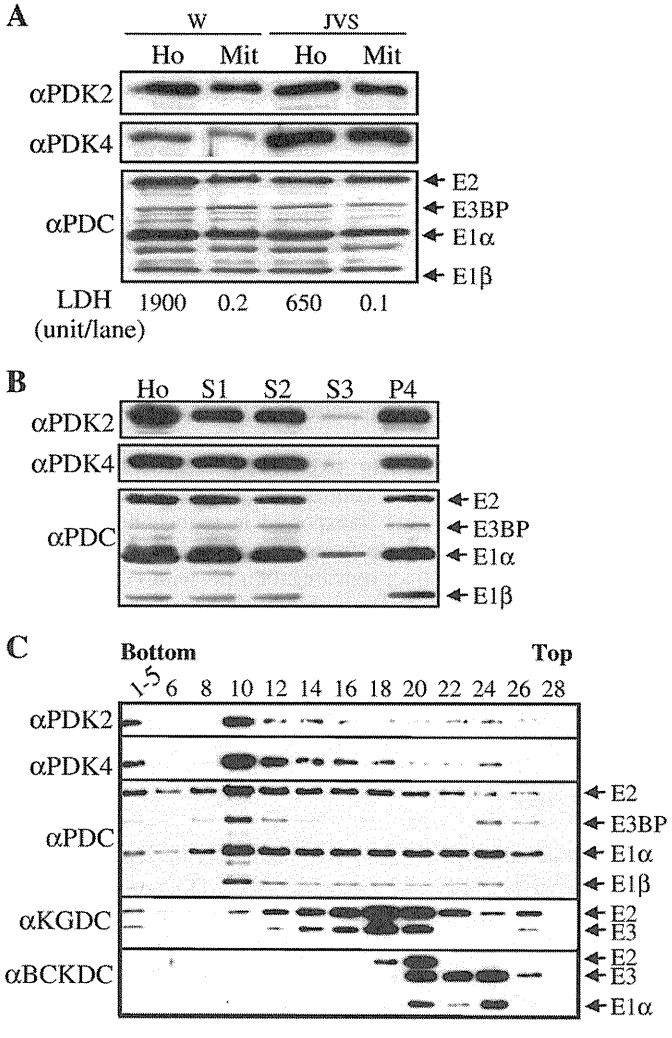

Fig. 3. Cellular distribution of PDK4 protein. (A) Levels of PDK2 and PDK4 proteins in homogenate (Ho) and mitochondrial (Mit) fractions by a sucrose gradient procedure (see Methods) are shown. Each lane contains the same CS activity (1.5 mU) representing the same mitochondria amount. Components (E2, E3BP, E1α and E1β) of PDC are detected and identified by anti-PDC antibody (αPDC). "LDH activity" means the degree of contamination of cytosolic components. (B) Each fraction (Ho, 6 μg; S1, 3 μg; S2, 2 μg; S3, 1 μg; P4, 1 μg of protein/lane) was analyzed by the respective antibodies (αPDK2, αPDK4 and αPDC). Ho, homogenate; S1, 600 ×*g* supernatant; S2, 20,000 ×*g* supernatant; S3, 100,000 ×*g* supernatant; P4, 100,000 ×*g* precipitation. (C) P4 fraction was fractionated with sucrose gradient centrifugation. PDK2, PDK4, PDC, KGDC (E2 and E3) and BCKDC (E2, E3 and E1α) were detected by the respective antibodies. The number corresponds to tube number fractionated from the bottom to top of the gradient.

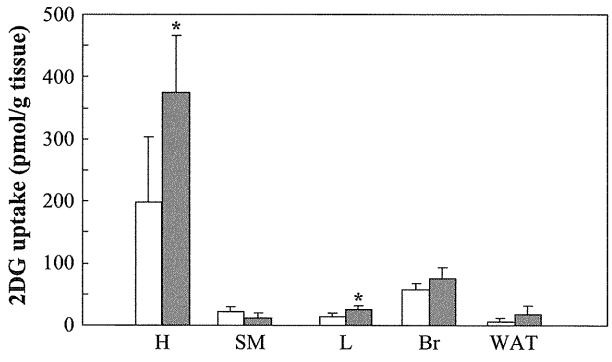

Fig. 4. Comparison of 2-DG uptake in tissues of control (open column) and JVS mice (gray column). Control and JVS mice under fed conditions were intraperitoneally injected with [^{3}H]2-DG. At 30 min after injection, the ^{3}H-radioactivity uptaken by the respective tissues, including the heart (H), skeletal muscle (SM), liver (L), brain (Br) and white adipose tissue (WAT) was measured (see Methods). Values are shown as the means ± SD ($n = 6$). * denotes $P < 0.05$ versus control mice.

PDC in fed JVS mice. In the literature, PDK4 protein itself has been considered to play an important role in inactivating PDC under physiological and pathological conditions [20,21,24–26]. Using PDK4 knock-out mice [45], PDK4 in tissues other than the liver has been shown to be important during fasting for regulation of PDC activity and glucose homeostasis [45]. However, our study has shown that there may be an underlying mechanism that increases PDK4 protein in the heart and skeletal muscle of JVS mice, but is less effective in suppressing PDC activity. As a possible mechanism, increased PDK4 protein may not fully interact with PDC in the mitochondria, resulting from an increase of the free form of PDK4. As shown in Fig. 3C, PDK4, as well as PDK2, appeared to be eluted in the fraction showing PDC, indicating that PDK4 binds physically to PDC. In the JVS heart, increased PDK4 was enriched in mitochondria, where it might interact with PDC (Fig. 3). For other PDK isoforms, the binding of PDK1-3 to PDC is influenced by the ratios of NADH to NAD and/or acetyl-CoA to CoA [27–29]. As a possible explanation, PDK4-PDC complex formation may be modulated intramitochondrially similar to other PDK-PDC complexes, depending on the values of [NADH/NAD] and/or [acetyl CoA/CoA] [27–29]. In carnitine-deficient tissues, disruption of fatty acid oxidation may result in low NADH/NAD and/or low acetyl CoA/CoA, which can affect the binding of PDK4-PDC. PDK4 has been thought to be regulated at the transcriptional step by fatty acids and/or hormones, including insulin and glucocorticoids [26,46,47]. Additionally, the present study supports that PDK4 is involved in PDC regulation at the post-transcriptional step as well as other PDKs [22,30]. Although it did not reveal the mechanism, the sucrose density gradient experiment demonstrated that PDK4 is tightly bound to the pyruvate dehydrogenase complex from the hearts of JVS mice. This is important because there is literature [28] indicating that PDK4 does not bind to the pyruvate dehydrogenase complex as tightly as the other PDKs.

We have reported that the respiratory quotient in fed JVS mice is greater than 0.9, which is similar to fed control mice, suggesting that carbohydrate is the main energy source [48]. In the present study, glucose transport was examined in control and JVS mice (Fig. 4). JVS mice showed significantly larger 2-DG uptake, corresponding to glucose uptake, in the liver and heart than the control. This finding is consistent with the other results obtained in this study showing that PDC is active in the heart and skeletal muscles of fed JVS mice (Table 1). This increased glucose uptake may compensate for the lower utilization of fatty acids in carnitine-deficient JVS mice. This assumption is consistent with previous reports on energy states in the heart and skeletal muscles in JVS mice [9,49]. These reports have noted that ATP levels are maintained even in the carnitine-deficient heart and skeletal muscles [9,49]. In the heart suffering from fatty acid oxidation abnormality due to carnitine deficiency, the preferential shift in energy from fatty acid to carbohydrate is required to suppress the atrophy of cardiac cells. Moreover, the increased uptake of glucose, which is induced in an insulin-dependent and/or -independent manner, may be involved in the development of cardiac hypertrophy [50]. Further studies are required to reveal the role of the increased glucose uptake in the development of cardiac hypertrophy. In the pressure-overloaded heart, another type of hypertrophy, decreased PDK4 protein, is associated with lowered suppression of PDC and enhanced glucose uptake, indicating that glucose oxidation is enhanced in place of fatty acid oxidation [20,21]. In hypertrophy due to carnitine deficiency, 2DG uptake, corresponding to glucose uptake, in the heart is also increased. This suggests that glucose utilization as a preferred energy source is a common mechanism developing cardiac hypertrophy of carnitine deficiency or pressure overload.

In conclusion, our data demonstrate that increased PDK4 protein in the adult fed carnitine-deficient mice does not significantly affect PDC inactivation, despite increased PDK4 protein in mitochondria. We have shown that PDC is a physiological substrate for PDK4 protein, based on co-fractionation of PDK4 protein with PDC as well as PDK2

protein. Further experiments are needed to clarify how PDC is protected from its inactivation and glucose uptake is enhanced, especially in the hypertrophied heart under carnitine deficiency.

Acknowledgments

We thank Drs. M. Itoh and Y. Kuroda (Tokushima University, Japan) for advice on the measurement of PDC activity, Drs. G. Yoshida and M.X. Li for valuable discussions, and Mr. D. Mrozek for editorial assistance. We are also grateful to Dr. R.A. Harris (Indiana University, IN) and Dr. Y. Shimomura (Nagoya Technical Institute, Japan) for supplying antibodies. This work was supported in part by Grants-in-Aid for Scientific Research (C-21590704 to M.H.) and by Special Coordination Funds for Promoting Science and Technology from the Ministry of Education, Culture, Sports, Science and Technology, the Japanese Government (T.S.).

References

[1] M. Horiuchi, H. Yoshida, K. Kobayashi, K. Kuriwaki, K. Yoshimine, M. Tomomura, T. Koizumi, H. Nikaido, J. Hayakawa, M. Kuwajima, T. Saheki, Cardiac hypertrophy in juvenile visceral steatosis (jvs) mice with systemic carnitine deficiency, FEBS Lett. 326 (1993) 267–271.

[2] K. Yoshimine, M. Horiuchi, S. Suzuki, K. Kobayashi, J.M. Abdul, M. Masuda, M. Tomomura, Y. Ogawa, H. Itoh, K. Nakao, M. Osame, T. Saheki, Altered expression of atrial natriuretic peptide and contractile protein genes in hypertrophied ventricle of JVS mice with systemic carnitine deficiency, J. Mol. Cell. Cardiol. 29 (1997) 571–578.

[3] M. Kuwajima, K. Lu, M. Sei, A. Ono, M. Hayashi, K. Ishiguro, K. Ozaki, K. Hotta, K. Okita, T. Murakami, J. Miyagawa, I. Narama, H. Nikaido, J. Hayakawa, H. Nakajima, M. Namba, T. Hanafusa, Y. Matsuzawa, K. Shima, Characteristics of cardiac hypertrophy in the juvenile visceral steatosis mouse with systemic carnitine deficiency, J. Mol. Cell. Cardiol. 30 (1998) 773–781.

[4] M.A. Jalil, M. Horiuchi, M. Nomoto, K. Kobayashi, T. Saheki, Catecholamine metabolism inhibitors and receptor blockades only partial suppress cardiac hypertrophy of juvenile visceral steatosis mice with systemic carnitine deficiency, Life Sci. 64 (1999) 1137–1144.

[5] M. Kuwajima, M. Horiuchi, H. Harashima, K. Lu, M. Hayashi, M. Sei, K. Ozaki, T. Kudo, H. Kamido, A. Ono, T. Saheki, K. Shima, Cardiomegaly in the juvenile visceral steatosis (JVS) mouse is reduced with acute elevation of heart short-chain acyl-carnitine level after L-carnitine injection, FEBS Lett. 443 (1999) 261–266.

[6] R. Takahashi, T. Asai, H. Murakami, R. Murakami, M. Tsuzuki, Y. Numaguchi, H. Matsui, T. Murohara, K. Okumura, Pressure overload-induced cardiomyopathy in heterozygous carrier mice of carnitine transporter gene mutation, Hypertension 50 (2007) 497–502.

[7] N. Longo, C. Amat Di San Filippo, M. Pasquali, Disorders of carnitine transport and the carnitine cycle, Am. J. Med. Genet. 142C (2006) 77–85.

[8] E. Gilbert-Barness, L.A. Barness, Pathogenesis of cardiac conduction disorders in children genetic and histopathologic aspects, Am. J. Med. Genet. 140A (2006) 1993–2006.

[9] M. Horiuchi, K. Kobayashi, M. Masuda, H. Terazono, T. Saheki, Pyruvate dehydrogenase kinase 4 mRNA is increased in the hypertrophied ventricles of carnitine-deficient juvenile visceral steatosis (JVS) mice, Biofactors 10 (1999) 301–309.

[10] T. Koizumi, H. Nikaido, J. Hayakawa, A. Nonomura, T. Yoneda, Infantile disease with microvesicular fatty infiltration of viscera spontaneously occurring in the C3H-H-2° strain of mouse with similarities to Reye's syndrome, Lab Anim. 22 (1988) 83–87.

[11] M. Kuwajima, N. Kono, M. Horiuchi, Y. Imamura, A. Ono, Y. Inui, S. Kawata, T. Koizumi, J. Hayakawa, T. Saheki, S. Tarui, Animal model of systemic carnitine deficiency: analysis in C3H-H-2° strain of mouse associated with juvenile visceral steatosis, Biochem. Biophys. Res. Commun. 174 (1991) 1090–1094.

[12] M. Horiuchi, K. Kobayashi, S. Yamaguchi, N. Shimizu, T. Koizumi, H. Nikaido, J. Hayakawa, M. Kuwajima, T. Saheki, Primary defect of juvenile visceral steatosis (jvs) mouse with systemic carnitine deficiency is probably in renal carnitine transport system, Biochim. Biophys. Acta 1226 (1994) 25–30.

[13] M. Horiuchi, K. Kobayashi, N. Asaka, T. Saheki, Secondary abnormality of carnitine biosynthesis results from carnitine reabsorptional system defect in juvenile visceral steatosis mice, Biochim. Biophys. Acta 1362 (1997) 263–268.

[14] K. Lu, H. Nishimori, Y. Nakamura, K. Shima, M. Kuwajima, A missense mutation of mouse OCTN2, a sodium-dependent carnitine cotransporter, in the juvenile visceral steatosis mouse, Biochem. Biophys. Res. Commun. 252 (1998) 590–594.

[15] J. Nezu, I. Tamai, A. Oku, R. Ohashi, H. Yabuchi, N. Hashimoto, H. Nikaido, Y. Sai, A. Koizumi, Y. Shoji, G. Takada, T. Matsuishi, M. Yoshino, H. Kato, T. Ohura, G. Tsujimoto, J. Hayakawa, M. Shimane, A. Tsuji, Primary systemic carnitine deficiency is caused by mutations in a gene encoding sodium ion-dependent carnitine transporter, Nat. Genet. 21 (1999) 91–94.

[16] T. Asai, K. Okumura, R. Takahashi, H. Matsui, Y. Numaguchi, H. Murakami, R. Murakami, T. Murohara, Combined therapy with PPARα agonist and L-carnitine rescues lipotoxic cardiomyopathy due to systemic carnitine deficiency, Cardiovasc. Res. 70 (2006) 566–577.

[17] M.A. Jalil, M. Horiuchi, M. Wakamatsu, M.X. Li, L. Begum, K. Suzuki, K. Kobayashi, T. Oka, T. Saheki, Attenuation of cardiac hypertrophy in carnitine-deficient juvenile visceral steatosis (JVS) mice achieved by lowering dietary lipid, J. Biochem. 139 (2006) 263–270.

[18] R. Takahashi, K. Okumura, H. Matsui, Y. Saburi, H. Kamiya, K. Matsubara, T. Asai, M. Ito, T. Murohara, Impact of α-tocopherol on cardiac hypertrophy due to energy metabolism disorder: the involvement of 1, 2-diacylglycerol, Cardiovasc. Res. 58 (2003) 565–574.

[19] G. Yoshida, M. Horiuchi, K. Kobayashi, M.D. Jalil, M. Iijima, S. Hagihara, N. Nagao, T. Saheki, The signaling pathway of cardiotrophin-1 is not activated in hypertrophied ventricles of carnitine-deficient juvenile visceral steatosis (JVS) mice, In Vivo 14 (2000) 401–405.

[20] M.E. Young, F.A. Laws, G.W. Goodwin, H. Taegtmeyer, Reactivation of peroxisome proliferator-activated receptor α is associated with contractile dysfunction in hypertrophied rat heart, J. Biol. Chem. 276 (2001) 44390–44395.

[21] A. Planavila, J.C. Laguna, M. Vázquez-Carrera, Nuclear factor-κB activation leads to down-regulation of fatty acid oxidation during cardiac hypertrophy, J. Biol. Chem. 280 (2005) 17464–17471.

[22] M.M. Bowker-Kinley, W.I. Davis, P. Wu, R.A. Harris, K.M. Popov, Evidence for existence of tissue-specific regulation of the mammalian pyruvate dehydrogenase complex, Biochem. J. 329 (1998) 191–196.

[23] J. Rowles, S.W. Scherer, T. Xi, M. Majer, D.C. Nickle, J.M. Rommens, K.M. Popov, R.A. Harris, N.L. Riebow, J. Xia, L. Tsui, C. Bogardus, M. Prochazka, Cloning and characterization of PDK4 on 7q21.3 encoding a fourth pyruvate dehydrogenase kinase isoenzyme in human, J. Biol. Chem. 271 (1996) 22376–22382.

[24] P. Wu, J. Sato, Y. Zhao, J. Jaskiewicz, K.M. Popov, R.A. Harris, Starvation and diabetes increase the amount of pyruvate dehydrogenase kinase isoenzyme 4 in rat heart, Biochem. J. 329 (1998) 197–201.

[25] Y.I. Kim, F.N. Lee, W.S. Choi, S. Lee, J.H. Youn, Insulin regulation of skeletal muscle PDK4 mRNA expression is impaired in acute insulin-resistant states, Diabetes 55 (2006) 2311–2317.

[26] P. Wu, J.M. Peters, R.A. Harris, Adaptive increase in pyruvate dehydrogenase kinase 4 during starvation is mediated by peroxisome proliferator-activated receptor α, Biochem. Biophys. Res. Commun. 287 (2001) 391–396.

[27] K.M. Popov, Regulation of mammalian pyruvate dehydrogenase kinase, FEBS Lett. 419 (1997) 197–200.

[28] A. Tuganova, I. Boulatnikov, K.M. Popov, Interaction between the individual isoenzymes of pyruvate dehydrogenase kinase and the inner lipoyl-bearing domain of transacetylase component of pyruvate dehydrogenase complex, Biochem. J. 366 (2002) 129–136.

[29] M. Kato, J.L. Chuang, S. Tso, R.M. Wynn, D.T. Chuang, Crystal structure of pyruvate dehydrogenase kinase 3 bound to lipoyl domain 2 of human pyruvate dehydrogenase complex, Embo J. 24 (2005) 1763–1774.

[30] R.M. Wynn, M. Kato, J.L. Chuang, S. Tso, J. Li, D.T. Chuang, Pyruvate dehydrogenase kinase-4 structures reveal a metastable open conformation fostering robust core-free basal activity, J. Biol. Chem. 283 (2008) 25305–25315.

[31] M. Horiuchi, K. Kobayashi, M. Tomomura, M. Kuwajima, Y. Imamura, T. Koizumi, H. Nikaido, J. Hayakawa, T. Saheki, Carnitine administration to juvenile visceral steatosis mice corrects the suppressed expression of urea cycle enzymes by normalizing their transcription, J. Biol. Chem. 267 (1992) 5032–5035.

[32] K.M. Popov, Y. Shimomura, R.A. Harris, Purification and comparative study of the kinases specific for branched chain α-ketoacid dehydrogenase and pyruvate dehydrogenase, Protein Expr. Purif. 2 (1991) 278–286.

[33] S. Matuda, T. Shirahama, T. Saheki, S. Miura, M. Mori, Purification and immunochemical studies of pyruvate dehydrogenase complex from rat heart, and cell-free synthesis of lipoamide dehydrogenase, a component of the complex, Biochim. Biophys. Acta 741 (1983) 86–93.

[34] J. Kirsch, J. Kuhse, H. Betz, Targeting of glycine receptor subunits to gephyrin-rich domains in transfected human embryonic kidney cells, Mol. Cell. Neurosci. 6 (1995) 450–461.

[35] P. Chomczynski, N. Sacchi, Single-step method of RNA isolation by acid guanidinium thiocyanate-phenol-chloroform extraction, Anal. Biochem. 162 (1987) 156–159.

[36] K.M. Popov, N.Y. Kedishvili, Y. Zhao, Y. Shimomura, D.W. Crabb, R.A. Harris, Primary structure of pyruvate dehydrogenase kinase establishes a new family of eukaryotic protein kinases, J. Biol. Chem. 268 (1993) 26602–26606.

[37] B. Huang, P. Wu, K.M. Popov, R.A. Harris, Starvation and diabetes reduce the amount of pyruvate dehydrogenase phosphatase in rat heart and kidney, Diabetes 52 (2003) 1371–1376.

[38] Y. Minokoshi, T. Alquier, N. Furukawa, Y. Kim, A. Lee, B. Xue, J. Mu, F. Foufelle, P. Ferre, M.J. Birnbaum, B.J. Stuck, B.B. Kahn, AMP-kinase regulates food intake by responding to hormonal and nutrient signals in the hypothalamus, Nature 428 (2004) 569–573.

[39] S.C. Dennis, M. DeBuysere, R. Scholz, M.S. Olson, Studies on the relationship between ketogenesis and pyruvate oxidation in isolated rat liver mitochondria, J. Biol. Chem. 253 (1978) 2229–2237.

[40] G.S. Denyer, D. Lam, G.J. Cooney, I.D. Caterson, Effect of starvation and insulin in vivo on the activity of the pyruvate dehydrogenase complex in rat skeletal muscles, FEBS Lett. 250 (1989) 464–468.

[41] H.G. Coore, R.M. Denton, B.R. Martin, P.J. Randle, Regulation of adipose tissue pyruvate dehydrogenase by insulin and other hormones, Biochem. J. 125 (1971) 115–127.

[42] G.J. Cooney, I.D. Caterson, E.A. Newsholme, The effect of insulin and noradrenaline on the uptake of 2-[1-^{14}C]deoxyglucose in vivo by brown adipose tissue and other glucose-utilising tissues of the mouse, FEBS Lett. 188 (1985) 257–261.

[43] Y. Ohira, S. Ishine, I. Tabata, H. Kurata, T. Wakatsuki, S. Sugawara, W. Yasui, H. Tanaka, Y. Kuroda, Non-insulin and non-exercise related increase of glucose utilization in rats and mice, Jpn J. Physiol. 44 (1994) 391–402.

[44] R.M. Moadel, A.V. Nguyen, E.Y. Lin, P. Lu, J. Mani, M.D. Blaufox, J.W. Pollard, E. Dadachova, Positron emission tomography agent 2-deoxy-2-[^{18}F]fluoro-D-glucose has a therapeutic potential in breast cancer, Breast Cancer Res. 5 (2003) R199–R205.